Formatted for *Genetics*

Genetic Basis of Aerobically Supported Voluntary Exercise: Results from a Selection Experiment with House Mice

David A. Hillis[1], Liran Yadgary[2,3], George M. Weinstock[4], Fernando Pardo−Manuel de Villena[2], Daniel Pomp[2], Alexandra S. Fowler[5], Shizhong Xu[6], Frank Chan[7], and Theodore Garland, Jr. [5]

[1] Genetics, Genomics, and Bioinformatics Graduate Program, University of California, Riverside, California 92521

[2] Department of Genetics, University of North Carolina at Chapel Hill, Chapel Hill, North Carolina 27599

[3] Present Address: Hazera Seeds Ltd. in Israel, Berurim M.P Shikmim, Israel 7983700

[4] The Jackson Laboratory for Genomic Medicine, Farmington, CT 06032

[5] Department of Evolution, Ecology, and Organismal Biology, University of California, Riverside, California 92521

[6] Depatment of Botany and Plant Sciences, University of California, Riverside, California 92521

[7] Friedrich Miescher Laboratory of the Max Planck Society, Tübingen, Germany

Running Title:
Genetics of aerobic voluntary exercise

Key Words:
artificial selection, behavior, complex traits, experimental evolution, population differentiation

Corresponding Author
Theodore Garland, Jr.
Department of Evolution, Ecology, and Organismal Biology
University of California, Riverside
Riverside, CA 92521
tgarland@ucr.edu
(951) 827-3524

Article Summary
House mice from 4 replicate lines selectively bred for 61 generations for voluntary wheel-running behavior were compared with 4 non-selected control lines using multiple genome-wide analytical techniques on both haplotype and single nucleotide polymorphism data. Twelve genomic regions were consistently found differentiated across all analytical approaches. These regions are associated with a diverse set of genes that appear related to exercise ability or motivational systems. Genes related to various organ systems (e.g. heart, brain) known to be physiologically different between test groups were identified. These results highlight candidate genes for detailed studies of exercise behavior and physiology.

ABSTRACT

The biological basis of exercise behavior is increasingly relevant for maintaining healthy lifestyles. Various quantitative genetic studies and selection experiments have conclusively demonstrated substantial heritability for exercise behavior in both humans and laboratory rodents. In the "High Runner" selection experiment, 4 replicate lines of *Mus domesticus* were bred for high voluntary wheel running (HR), along with 4 non-selected control (C) lines. After 61 generations, the genomes of 79 mice (9-10 from each line) were fully sequenced and single nucleotide polymorphisms (SNPs) were identified. We used nested ANOVA with MIVQUE estimation and other approaches to compare allele frequencies between the HR and C lines for both SNPs and haplotypes. Approximately 61 genomic regions, across all somatic chromosomes, showed evidence of differentiation. Twelve of these regions were differentiated by all methods of analysis. Gene function was inferred largely using Panther gene ontology terms and KO phenotypes associated with genes of interest. Some of the differentiated genes are known to be associated with behavior/motivational systems and/or athletic ability, including *Sorl1, Dach1*, and *Cdh10*. Sorl1 is a sorting protein associated with cholinergic neuron morphology, vascular wound healing, and metabolism. *Dach1* is associated with limb bud development and neural differentiation. *Cdh10* is a calcium ion binding protein associated with phrenic neurons. Overall, these results indicate that selective breeding for high voluntary exercise has resulted in changes in allele frequencies for multiple genes associated with both motivation and ability for endurance exercise, providing candidate genes that may explain phenotypic changes observed in previous studies.

INTRODUCTION

Most traits of interest in biology are complex, modulated by numerous genetic and environmental factors, and comprised of multiple lower-level (subordinate) traits that often influence higher-level traits in nonintuitive ways (Garland *et al.* 2016; Sella and Barton 2019). Examples of complex traits include human height, which is influenced by more than 9,500 quantitative trait loci (QTL) (Wood *et al.* 2014), as well as one's susceptibility to various psychological diseases (Horwitz *et al.* 2019).

One complex trait of great interest to medicine is exercise behavior. Exercise has been linked to numerous health benefits, including muscle and bone strength, weight control, reduced cardiac disease, and improved mental health (Manley 1996; Lightfoot *et al.* 2018). Nonetheless, the majority of Americans are not getting sufficient exercise and this problem is common world-wide (Guthold *et al.* 2018). Not only does insufficient exercise contribute to such health issues as obesity and diabetes (Booth *et al.* 2002; Cornier *et al.* 2008; Myers *et al.* 2017), but it also increases healthcare costs in the United States, e.g., by more than $100 billion annually between the years of 2006-2011 (Carlson *et al.* 2015). Conversely, higher levels of physical activity promote physical fitness and cardiovascular health, while lowering risk for depression, anxiety-related disorders, obesity, Type 2 diabetes, and mortality (Blair and Morris 2009; Matta Mello Portugal *et al.* 2013; Mok *et al.* 2019).

The health benefits of exercise occur by various mechanisms (Neufer *et al.* 2015), as do the adverse effects of a lack of exercise (Booth *et al.* 2012). Acute exercise can have beneficial effects on immune function (Sellami *et al.* 2018) and cognition (Park and Etnier 2019). Chronic exercise training can cause changes in muscle fiber type composition that benefit regulation of

energy metabolism and other metabolic pathways (Fan *et al.* 2013). Furthermore, exercise has been linked to lower blood pressure by reducing systemic vascular resistance (Cornelissen and Fagard 2005). Reduced blood pressure, in turn, reduces risk of cardiac disease (Benjamin *et al.* 2019). The release of endorphins and vascular endothelial growth factors have shown promise as explanations for the growth of new neurons in the brain, which may be the cause of reduces symptoms of neurological diseases such as depression (Ernst *et al.* 2006).

Identifying genetic determinants of exercise behavior could potentially lead to drug targets that would help promote motivation for exercise and/or benefits derived from exercise. Additionally, by identifying genetic causes of motivation for exercise we may also gain insight regarding higher-level structures or pathways that control this motivation. A variety of human studies have been conducted to determine the genes or chromosomal regions that modulate various components of exercise behavior, including both motivation and/or capability to exercise (Lightfoot *et al.* 2018). Many of these studies use observational methods to compare humans who engage in either frequent and/or strenuous exercise with those who are less active (Kostrzewa and Kas 2014; Lin *et al.* 2017). Historically, the most common approach to measuring human exercise levels was by use of questionnaires, which can be of dubious reliability, but an increasing number of studies use accelerometers (Prince *et al.* 2008; Dyrstad *et al.* 2014). Detecting QTL in these studies is generally done with genome-wide association studies (GWAS), which rely on phenotypic and genetic data from many individuals within a population and can identify particularly strong correlations between the phenotype and key genetic markers and loci.

Various QTL identified in humans are associated with motivation, e.g., dopaminergic

127 regulation. Dopamine is a well-established modulator of exercise motivation or reward
128 (Garland *et al.* 2011b). Various genes associated with the dopamine pathway are associated
129 with exercise behavior in humans (Simonen *et al.* 2003; Loos *et al.* 2005; De Moor *et al.* 2009).
130 The large body of evidence that dopamine signaling is a major component of exercise
131 motivation dwarfs other motivational systems that have been associated with exercise,
132 including serotonin and endocannabinoids (Dietrich 2004; Cordeiro *et al.* 2017), though
133 serotonin has been implicated in GWAS of hyperactivity disorders (Aebi *et al.* 2016).
134 Other human studies have detected QTL associated with physical traits related to
135 exercise abilities, including maximal oxygen consumption (VO_{2max}) (Williams *et al.* 2017), bone
136 density (Herbert *et al.* 2019), and more (Lin *et al.* 2017). The list of possible biological traits
137 affiliated with exercise and their associated QTL is extensive (Sarzynski *et al.* 2016; Lightfoot *et*
138 *al.* 2018).
139 Observational studies of human exercise behavior are limited by measurement error
140 and environmental cofactors that cannot always be accounted for in statistical models
141 (Garland *et al.* 2011b; Lightfoot *et al.* 2018). One alternative is to use animal models derived
142 from selective breeding experiments (Garland and Rose 2009). Selective breeding will alter the
143 proportions of alleles that affect a trait of interest, thus allowing for easier detection of such
144 alleles (Britton and Koch 2001; Konczal *et al.* 2016). Finding the genetic factors that underlie a
145 complex trait is also facilitated by reducing environmental variation ("noise"), as is possible with
146 laboratory colonies of rodents (Parker and Palmer 2011).
147 To elucidate the biological basis of voluntary aerobic exercise behavior, a selection
148 experiment was begun in 1993 using a base population of outbred Hsd:ICR mice. Four replicate

lines have been bred for high voluntary wheel-running behavior and another four bred without regard to their wheel running as controls for founder effects and random genetic drift (Swallow *et al.* 1998). Since the beginning of this experiment, over 150 papers have been published that document a variety of phenotypic differences between the High Runner (HR) and Control (C) lines. These previous studies establish morphological and physiological differences in bone, kidney, heart, skeletal muscle, brain, and other organs and systems (Rhodes *et al.* 2005; Swallow *et al.* 2005; Kolb *et al.* 2013b; Wallace and Garland 2016) and, more generally, reaffirm the diversity of the systems involved in voluntary exercise behavior (Garland *et al.* 2011b; Lightfoot *et al.* 2018). The previous studies also give potential directions for informed analyses of the genome. For example, we would expect divergence in allele frequencies related to the reward system in the brain and to muscle function. The HR selection experiment is the world's "largest" involving a behavioral trait in rodents in terms of the number of lines and generations. Therefore, addressing the genomic differences between the HR and C mice is expected to provide novel insights into the underpinnings of exercise behavior.

Previously, Xu and Garland (2017) used a mixed model (nested ANOVA) with minimum variance quadratic unbiased estimation (MIVQUE) to analyze medium-density single nucleotide polymorphism (SNP) data for the HR and control lines sampled from generation 61 (Xu and Garland 2017). This statistical method proved more powerful than the commonly used regularized F test and Generalized Linear Mixed Model (GLMM) methods when incorporating permutation-based multiple testing correction. The data used included 7-10 females from each of eight lines (four HR and four C). Genotypes were determined with the MegaMUGA SNP-chip (Morgan and Welsh 2015). After removing markers with missing data, 25,318 markers were

analyzed with the mixed models, finding 152 markers to be significantly differentiated between the HR and C linetypes (i.e. test group). Although Xu and Garland (2017) demonstrated numerous SNP loci with evidence of differentiation between the HR and control lines, biological interpretations were not presented. Additionally, as demonstrated by the whole-genome sequence (WGS) data addressed in this paper, various differentiated loci were not detected in the previous SNP-chip analysis.

Here, we apply the mixed model with MIVQUE estimation method to WGS data obtained from the same individuals as in Xu and Garland (2017). We analyze both SNP and haplotype data to take full advantage of the information provided by each data type (Shim *et al.* 2009; Taliun *et al.* 2016). We also use simulations to explore some of the statistical properties of the MIVQUE estimation method for this application, and we implement procedures aimed at improving model fit and potentially statistical power. We identify numerous SNP and haplotype loci as potential candidates for functionally relevant genetic differentiation between the HR and C lines. Many of these can be tied to specific lower-level traits that should influence exercise behavior, through use of gene ontology terms and KO phenotype analyses of nearby genes.

Using information on known morphological and physiological differences between the HR and control lines, we were able to perform both broad and directed strategies to detecting significantly differentiated loci. We show that the method of Xu and Garland (2017) can be improved by allowing for different among- and within-line variance structures. We identified several potentially differentiated genes associated with bone, heart, and brain morphology. We also identified a few candidates with potential large-scale influences on the HR mice,

including *Sorl1, Dach1*, and *Cdh10*.

MATERIALS AND METHODS

High Runner Mouse Model

As described previously (Swallow *et al.* 1998; Careau *et al.* 2013), 112 males and 112 females of the outbred Hsd:ICR strain were purchased from Harlan Sprague Dawley in 1993. These mice were randomly bred in our laboratory for 2 generations. Ten males and 10 females were then randomly chosen as founders for each of 8 closed lines (generation 0). Four of these lines were randomly picked to be "High Runner" (HR) lines, in which mice would be selected for breeding based on voluntary wheel running. The remaining 4 lines were used as Control (C) lines, without any selection. At approximately 6-8 weeks of age, all mice were given access to wheels for six days. The amount of running (total revolutions) on days 5 and 6 was used as the selection criterion. For the non-selected C lines, one male and one female from each of 10 families were chosen as breeders to propagate the line. For the HR lines, the highest-running male and female from within each of 10 families were chosen as breeders (within-family selection). Sib-mating was disallowed in all lines (Swallow *et al.* 1998).

Whole-genome Sequencing

DNA was collected from 80 mice (10 from each line), from generation 61, via phenol-chloroform extraction and sequenced on an Illumina HiSeq 2500 1T platform. Libraries were constructed using Nextera kit and reads were trimmed and aligned to the GRCm38/mm10 mouse genome assembly as described in Didion et al. (2016). This generated an average read depth of 12X per mouse. SNPs were filtered based on genotype quality ("GQ") >5, read depth >3, MAF <0.0126 for all samples, and Mapping Quality ("MQ") >30. One of the 80 mice was

excluded due to likely contamination (as in Xu and Garland 2017), leaving 79 for the following analyses. SNPs not found to be present in at least two of the 80 mice were also removed from analysis. Although Xu and Garland (2017) had identified these as females, they were in fact all males with exception of one female from line 5.

Heterozygosity Calculations

Individual mouse heterozygosity (multi-locus heterozygosity) was calculated by dividing the number of heterozygous loci for each mouse by the total number of segregating loci across all 80 mice (n=5,932,124). Heterozygosity per line is the average of the heterozygosity of all sequenced mice within that line.

SNP Analysis

Individual Single Nucleotide Polymorphisms (SNPs) were initially analyzed using a mixed model approach with the Minimum Variance Quadratic Unbiased Estimation of variance (MIVQUE) method of estimating variance parameters as described in Xu and Garland (2017). However, rather than removing loci or mice (which had been necessary in the Xu and Garland paper, resulting in 7-10 mice per line analysed) with missing data, code was modified to remove only the missing values themselves. The MIVQUE analysis provides a p-value for each locus for rejecting the null hypothesis of no differentiation between the HR and C lines. Xu and Garland had performed the analysis using two different encoding schemes to represent genotypes as 0, 0.5 and 1 vs. as twin vectors of 0-0, 0-1 and 1-1. We have since determined that the twin vectors encoding was preferable, and we report only those results (File S7).

Multi-Model Analysis of SNP Data from Whole-genome Sequences

The analyses performed in Xu and Garland (2017) used a single statistical model in R for all loci

(our comparable SAS model being "Simple" in Table 1). This model did not allow for several possibilities that might be expected a priori and that were in fact observed, such as differing variances among the 4 replicate HR and C lines (designated “SepVarLines” in Table 1), as is the case for wheel-running behavior (Garland *et al.* 2011a). Beyond this, the amount of variation among individual mice within the replicate lines might differ for the HR and C lines (“Full” model). Interpretation of these different models is presented in the Discussion. In total, we applied four alternate models to the data for each locus, and followed a model selection procedure for the one with the lowest the Aikake Information Criterion, corrected for small sample sizes (AICc), and retained the p-value for its linetype effect (differentiation between the HR and C lines). All Multi-Model analyses were performed in SAS using PROCEDURE MIXED with the mivque0 method (File S10). We elected to prioritize SAS over R for its performance gains over large number of loci. For a direct comparison, we reanalyzed the MegaMUGA data in Xu and Garland (2017) the multi-model method (Figures S1 and S2).

Loci that contained no within-line variance (i.e. each line was fixed for one allele or the other) could not be analyzed with the foregoing procedures. We analyzed these loci by counting the net number of alternatively fixed lines among the HR and C linetypes. Those loci with greater difference in allele frequency between the HR and C linetypes are regarded as being more “significant.”

Table 1 Summary of covariance models

Model	d.f.	Covar-iance Param-eters	Description	HR and C different among-line variance	HR and C different within-line variance	HR and C same among-line variance	HR and C same within-line variance	SAS Code

Full	6	4	Random effects for replicate line within selection treatment (linetype) and for mouse within line and linetype, allowing for separate variance estimates for both lines within linetype and mouse within line and linetype	**x**	**x**			proc mixed data=locus method=mivque0;
								class pop sub mouse;
								model COL1 =pop/solution;
								random sub(pop) /group=pop;
								random mouse(sub pop) /group=pop;

SepVarLines	6	3	Random effects for replicate line within selection treatment (linetype) and for mouse within line and linetype, allowing for separate variance estimates for line within linetype	**x**			**x**	proc mixed data=locus method=mivque0;
								class pop sub mouse;
								model COL1=pop/solution;
								random sub(pop) /group=pop;
								random mouse(sub pop);

SepVarInd	6	3	Random effects for replicate line within selection treatment (linetype) and for mouse within line and linetype, allowing for separate variance estimates for mouse within line and linetype		**x**	**x**		proc mixed data=locus method=mivque0;
								class pop sub mouse;
								model COL1=pop/solution;
								random sub(pop);
								random mouse(sub pop) /group=pop;

Simple	6	2	Random effects for replicate line within selection treatment (linetype) and for mouse within line and linetype (as used by Xu and Garland 2017)			**x**	**x**	proc mixed data=locus method=mivque0;
								class pop sub mouse;
								model COL1=pop/solution;
								random sub(pop);
								random mouse(sub pop);

Multiple models[a] used to analyze the allelic SNP data (two values per mouse) for whole-genome sequences from 79 mice. For each model, we used SAS Procedure Mixed with MIVQUE estimation (Xu and Garland 2017) to obtain the test statistic (F), significance level (P), and AICc (d.f. method was containment).

[a] For some loci, the within-line variance was zero for all 8 lines. In those cases, we used direct enumeration to calculate a significance level, i.e., the probability of observing the pattern versus the 23 possible combinations. See text for further details.

Table 2 Basic descriptive statistics for the primary analyses

Dataset	Total "Loci"	Significant Loci	Critical Threshold	Significant Genes
MegaMUGA	25,332	162[a]	p<0.00526 (5% FWER)	174[b]
Whole-Genome SNPs	5,932,124	84	p<0.001 (Local Maximum)	27
Haplotypes	16,901	102[c] (28 regions)	p<0.00526 (See text)	154[b]
All HR Fixed, All C Polymorphic	5,932,124	2,562 (46 regions)	See text	135[b]

[a]In Xu and Garland (2017), 152 SNPs were identified as statistically significant with a single model and the MIVQUE procedure, after use of a permutation procedure to control the family-wise Type I error rate (FWER) at 5% ($p < 0.00343$).

[b]These are not genes that SNPs fell into. These are genes close to significant SNPs or haplotypes.

[c]From 28 closely linked groups.

Multiple Testing Correction

Permutations for MegaMUGA Data

This approach is based on the permutation method used by Xu and Garland (2017), but modified to account for the multiple models. All permutations were performed using SAS PROC MIXED as described above in the section on multi-model approach. The mouse IDs, line, and linetype were randomly permuted as a block to break their original associations with the allelic data but not with each other. The permuted data for each locus were then analyzed with each of the four models listed in Table 1 (i.e., for the MegaMUGA SNP data, 4 X 25,332 analyses were performed). For each of the four models, the AICc was recorded, and the corresponding F-statistics were retained. From these 25,332 loci (for the MegaMUGA data), the F-statistic corresponding to the model with the lowest AICc was saved. The foregoing process was repeated 5,000 times, the resulting F-statistics were sorted from largest to smallest, and the 250th largest F-statistic was used to establish the critical value for the 5% FWER.

Permutations for Haplotype Data

Permutations done for haplotypes were performed separately for 2-allele haplotype blocks and 3-allele blocks, using 1,000 permutations to keep computational times manageable. As in the unpermuted haplotype analyses, blocks with three alleles (n=5,869) were analyzed with two dummy variables, each individual dummy variable was tested using the multi-model method, and the two p-values generated were combined using Fisher's method (Fisher 1925). However, some permutations of the 3-allele blocks produced erroneous low p-values (apparently due to numerical issues), which, if included in subsequent calculations would have caused an artifactual reduction of the critical value needed to obtain the true 5% FWER. The

permutations of the 2-allele blocks (n=11,032) did not produce any artifactually low p-values. Given the problems with the 3-allele haplotype permutations, we elected to apply the MeguMUGA permutation threshold (P<0.00526) to the haplotype blocks because of their similar sample size (MegaMUGA=25,332; Haplotypes=16,901) and the fact that they should be highly correlated.

Local Maxima Selection for WGS Data

In the original paper, which analyzed 25,332 SNPs from a commercial chip, a permutation procedure was used to control the family-wise Type I error rate (FWER) at 5% (Xu and Garland 2017). Those procedures were not computationally practical for the 5,932,124 SNPs from the whole-genome sequences, nor are linked SNPs within a haplotype block truly independent from each other. Accordingly, significant loci were chosen via a combination of -logP cutoff and local maximum (LM) determination, the latter acting as a filter to focus on actual selected loci over their hitchhikers. Similar methods have been previously described (Nicod *et al.* 2016). Briefly, suggestive loci with -logP >3.0 were clustered with a maximum gap of 1 Mbp. For each such cluster, the global peak, and a set of local maxima were determined for every 500 kbp spanned by the cluster. The set of local maxima were chosen as peaks separated by dips in the signal below the median -logP in the cluster. These LM SNPs were annotated using R libraries GenomicFeatures and VariantAnnotation, with the mm10 knownGene.sqlite database provided by the Genome Browser team at the University of California, Santa Cruz.

Haplotype Determination

From the whole-genome sequences, haplotypes were determined using JMP 11 and JMP Scripting Language (SAS Institute Inc., Cary, NC). To construct haplotypes, we first defined the

304 genomic block segments as consecutive 20 kbp windows that did not transition between
305 homozygous and heterozygous states. For each block region, we performed a hierarchical
306 clustering analysis using SNP genotype data (of homozygous regions only) as input. Preliminary
307 haplotype analysis showed that the HR population at generation 61 rarely had more than 3
308 alleles in a given haplotype. Therefore, the analysis was restricted to a maximum of three
309 clusters (haplotype alleles) per block (File S5).

310 ## Haplotype Analysis

311 As for the SNP data, haplotype data were analyzed using the multi-model method described
312 above. Haplotype blocks with only two alleles (n=11,032) were analyzed the same way as for
313 the SNP data (File S10). Blocks with three alleles (n=5,869) were analyzed with two dummy
314 variables, with the base allele chosen as the most common one, and then two dummy variables
315 coding for presence of the other two alleles. Each individual dummy variable was tested using
316 the multi-model method. The two p-values generated from the two dummy variables were
317 combined using Fisher's method (Fisher 1925). Different models potentially were used for each
318 dummy variable based on AICc, allowing for up to two models to contribute to the final p-value
319 of a locus (File S6).

320 ## SNPs Fixed in One Treatment but Polymorphic in the Other

321 As noted previously with the SNP chip data (Xu and Garland 2017), we observed no loci that
322 were fixed for one allele in all four HR lines while being fixed for the alternate allele in all four C
323 lines (see Results). We did, however, observe loci fixed for a given allele in all 4 HR lines, which
324 is symptomatic of a complete selective sweep (caused by directional selection) as described by
325 Burke (2012), while remaining polymorphic in all 4 C lines. All loci that were fixed in the HR

mice and simultaneously polymorphic in all C lines (FixedHR/PolyC) were extracted from the multi-model results and grouped such that those fixed loci that were within 100,000 bp of other fixed loci would be part of the same group. This process was then repeated for loci fixed in the Control lines but polymorphic in all HR lines (FixedC/PolyHR).

General Ontology Analysis

Transcribed regions (N = 56, as indicated in Table 2) found to contain LM based on the whole-genome sequence analyses were analyzed using The Gene Ontology Resource (GO). GO analyses were performed based on biological process, molecular function, and cellular component. Ontologies reported as significant at raw $p < 0.05$ for any of these three categories are reported here. Analysis of these genes was also performed using the Database for Annotation, Visualization and Integrated Discovery (DAVID). The results of these analyses did not vary greatly from the GO results.

Targeted Ontology Analysis

Previous papers show that the HR lines of mice have diverged from the C lines for many different phenotypes (reviews in Rhodes *et al.* 2005; Garland *et al.* 2011b; Wallace and Garland 2016). Many of these phenotypes can be tied to specific neurobiological or physiological functions. In such cases, a logical approach is to analyze separately some candidate genes known to be affiliated with relevant functions and find differentiated SNPs for those genes. We used this approach for several ontologies. Specifically, lists of genes affiliated with dopamine, serotonin, brain, bone, cardiac muscle, and skeletal muscle were extracted from the Mouse Genome Informatics website. SNPs found within these genes were separated from the full WGS data and the most differentiated among these were recorded.

Data Availability Statement

Any additional intermediary or results file are available upon request. Supplemental files are available at FigShare. File S1 contains supplemental figures and brief descriptions of all other supplemental files and tables. File S2 contains allelic SNP data. File S3 contains mouse data with line and lintype. File S4 contains all results for analyses of individual SNPs. File S5 contains all haplotype data. Files S6 contains all results for analyses of haplotype data. File S7 contains justification for use of allelic coding of alleles. File S8 includes simulations of Type I error rates for Mixed Model analyses using MIVQUE variance estimation. File S9 expands on the discussion of genes in consistent regions (see Results). File S10 includes all R and SAS code used for the SNP and haplotype analyses. Table S1 includes local maxima associated genes. Table S2 contains groups of loci fixed in all lines of one lintype but polymorphic in all lines of the other. Table S3 includes heterozygosity for each individual mouse. Table S4 includes top ten genes for each of the targeted ontologies analyses. Table S5 includes allele frequency by line of each loci identified as a local maximum. Table S6 includes genomic regions identified as suggestive ($p<0.001$) by the SNP analyses.

RESULTS

Variation in Genetic Diversity

After 61 generations of the High Runner mouse selection experiment, and based on a sample of 79 mice, we found SNPs segregating at 5,932,124 loci (~2.2 SNPs per kbp or 0.22%) across the entire set of lines (i.e., at least 2 mice containing an alternate allele were found across the 79 mice sequenced) with at least 1.5% minor allele frequency. Individual lines contained 2.04 – 2.82M SNPs (34–48% of the total diversity) (Table 3), with no appreciable loss in diversity for the HR lines compared to the Control replicates (Mann-Whitney U-test, W=6; p-value=0.6857). SNP heterozygosity ranged from 10.3% to 20.6% among individual mice (Table S3) and averaged 12.7% to 18.1% per line (Table 3).

Table 3 Summary of polymorphism and heterozygosity by line

Line	Polymorphic SNP loci	SNP %	Polymorphic Haplotypes	Haplotype %	SNP Het	Haplotype Het
C1	2,333,951	39.3%	7,773	46.0%	14.7%	17.8%
C2	2,436,225	41.1%	7,652	45.3%	13.7%	16.6%
C3	2,602,007	43.9%	7,841	46.4%	15.8%	17.8%
C5	2,102,405	35.4%	7,160	42.4%	12.7%	16.5%
HR3	2,819,828	47.5%	8,717	51.6%	18.1%	19.6%
HR6	2,220,487	37.4%	7,060	41.8%	13.5%	16.2%
HR7	2,042,309	34.4%	6,304	37.3%	13.0%	14.7%
HR8	2,226,282	37.5%	7,315	43.3%	14.4%	16.6%

Initial haplotype analysis demonstrated that there were rarely more than three alleles for any given haplotype block (region with little to no discernable recombination events within the 79 mice analyzed). Therefore, for the final haplotype analysis, hierarchical clustering was performed with a limit of 3 clusters. 16,901 of these blocks remained variable across the 8 lines

in generation 61. As would be expected, the number of haplotypes that have not gone to fixation in each line appears to be proportional to the number of SNPs that have not gone to fixation (Table 3). Heterozygosity for the haplotypes ranged from 12.2% to 25.5% for individual mice (Table S3), and 14.7% to 19.6% when averaged per line (Table 3). Heterozygosity for the haplotype data were not significantly different between HR and C lines (Mann-Whitney U-test, W=8; p-value=1.0 and W=6; p-value=0.6857, respectively).

Multi-Model vs Single-Model Comparisons

As expected, we found that many, indeed most, loci were better fit by models other than the "Simple" model used by Xu and Garland (2017). Generally, the “Full” model was the most preferred, followed by the “Simple” model (Table 4). In general, differences between the p-values determined by the single and multi-model methods were negligible (Figure S2).

When analyzing data generated under the null hypothesis, the mixed models with MIVQUE estimation for both single and multi-model produced a deflated Type I error rate for α = 0.05 (File S8). The multi-model approach helped to correct this, but the Type I error rate did not improve greatly with the multi-model approach alone. We attempted to utilize the Kenward Rogers method of determining degrees of freedom to correct this low Type I error rate, but this did not bring Type I error rate to 0.05 and effectively dropped the nested line effect for many loci. We did not want to drop the nested line effect because this ignores the fundamental experimental design of the selection experiment. However, the permutation and local maxima methods of determining loci of interest are robust to this deflated Type I error rate (File S8), so we proceeded with our analyses using conservative results produced by the MIVQUE variance estimation method.

Table 4 Model preference by data set, test, and allele counts

Model	MegaMUGA[a]	WGS[a]	Hap 2-allele[b]	Hap 3-allele[b]
Full	9,875 (39.0%)	2,441,601 (41.2%)	4,512 (40.9%)	5,510 (46.9%)
SepVarLine	3,105 (12.3%)	504,946 (8.5%)	1,052 (9.5%)	1,583 (13.5%)
SepVarInd	2,983 (11.8%)	716,265 (12.1%)	726 (6.6%)	748 (6.4%)
Simple	8,654 (34.2%)	2,186,803 (36.9%)	4,594 (41.6%)	3,615 (30.8%)
# with no within-line variance	715 (2.8%)	82,533 (1.4%)	148 (1.3%)	282 (2.4%)

[a]Number of SNPS whose lowest AICc match the indicated model

[b]Number of haplotype blocks whose lowest AICc match the indicated model (one for each dummy variable for 3-allele blocks)

Three Major Analyses

Whole-Genome Haplotype

No haplotypes were identified as being fixed in all HR lines for one allele and fixed in all C lines for the opposite allele. The multi-model haplotype analysis produced 102 blocks of significant differentiation at the p<0.005 (permutations) level. Significant blocks could be found on 13 chromosomes (Figure 1). We consider haplotype blocks within 1,000,000 bp of each other to be linked and therefore part of the same haplotype group: 28 such groups were determined (Table 5). These groups include a total of 154 transcribed sequences recognized by the Panther database for gene ontology. The largest of these groups was found on chromosome 14:52,100,155-54,334,868 bp (Table 5).

Figure 1 Manhattan plot for haplotype data. Red line indicates p-value <0.005 (see Methods and Materials), which yielded 28 haplotype groups (see Table 5).

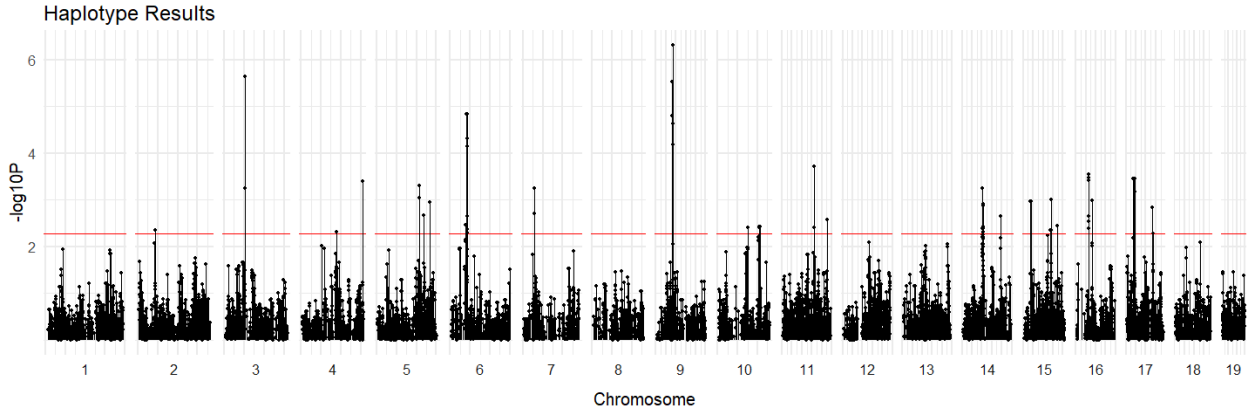

Table 5 Significant haplotype groups

Group	Chr	Start (BP)	End (BP)	Size (BP)	P-value
1	2	43,100,041	43,214,647	114,606	4.42E-03
2	3	51,580,020	51,659,891	79,871	2.25E-06
3	4	89,300,145	89,357,884	57,739	4.92E-03
4	4	155,480,343	155,654,426	174,083	3.94E-04
5	5	108,000,623	108,679,807	679,184	4.85E-04
6	5	118,824,587	119,299,787	475,200	2.15E-03
7	5	132,540,807	133,720,551	1,179,744	1.12E-03
8	6	37,440,411	37,659,588	219,177	3.47E-03
9	6	41,584,862	43,431,434	1,846,572	1.47E-05
10	7	29,640,243	29,697,093	56,850	5.67E-04
11	9	41,240,184	42,275,833	1,035,649	4.90E-07
12	10	75,061,742	75,456,261	394,519	3.99E-03
13	10	103,363,232	104,139,953	776,721	3.94E-03
14	10	105,220,041	105,699,704	479,663	3.72E-03
15	11	79,724,263	81,409,849	1,685,586	1.89E-04
16	11	114,466,946	114,489,018	22,072	2.69E-03
17	14	52,100,155	54,334,868	2,234,713	5.62E-04
18	14	98,380,090	98,679,965	299,875	2.22E-03
19	15	18,960,135	19,759,996	799,861	1.09E-03
20	15	69,120,025	70,219,737	1,099,712	4.53E-03
21	15	71,480,090	71,559,595	79,505	9.91E-04
22	15	86,541,805	86,599,823	58,018	3.55E-03
23	16	31,540,757	33,178,952	1,638,195	2.79E-04
24	16	40,742,298	41,357,426	615,128	1.01E-03
25	17	18,020,933	18,039,390	18,457	3.54E-04
26	17	20,700,046	20,939,819	239,773	3.54E-04
27	17	23,000,233	23,599,776	599,543	3.54E-04
28	17	65,458,617	65,738,255	279,638	1.46E-03

Whole-Genome SNP

Similarly to haplotypes, no individual SNPs were identified as being fixed in alternative alleles across all HR on one hand and all C lines on the other. At the p<8.4E-09 critical level (Bonferroni-corrected), only two SNPs in chromosome 5 were identified to be significantly differentiated across the entire genome (Figure 2), both in an intron of an uncharacterized gene (GM34319). The syntenic/orthologous region of both the human and cat genomes correspond to a coding region (exon 3) of the MYL5 gene (Myosin light chain 5). Due to the small number of significant SNPs under Bonferroni and the computational difficulties of using permutations with the multi-model method, we focus on local maxima SNPs.

Figure 2 Manhattan plot for WGS SNP data. Red dots represent local maxima (N = 84).

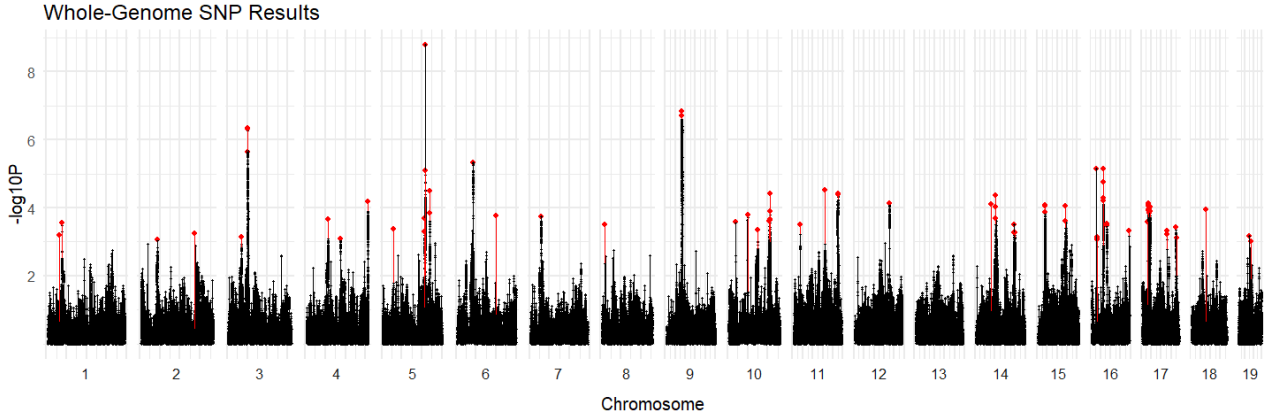

In the local maxima (LM) analyses, the suggestive cutoff (-logP>3.0) produced 38,065 SNPs for analysis. 44 clusters were found, ranging in size from 1 SNP to 3,787 SNPs (Chr9: 41,303,824-42,478,817 bp). The largest single group in terms of genome spanned is on chr17: 17,846,983-23,586,163 bp (Table 6). From these groups, a total of 84 LM were determined. 31 of these SNPs were associated with 27 unique transcribed regions. 26 of the 27 genes could be

utilized for GO analysis. Although chromosome 3 had no LM fall into specific genes (despite clear significance based on the Manhattan plot), the cluster on chr3 (chr3:51,190,735-52,498,029 bp) includes about 10 validated coding genes and various predicted genes, but none of the LMs fall in these. However, all three LMs in this group are upstream of Setd7, a methyltransferase.

The most significant SNPs with no within-line variance fell into three regions. One of these regions is on chromosome 5 (105-109 mbp), which is close to the LM identified in this chromosome. Another is on chromosome 16 (44 mbp), about 2.5 million base pair from the LM on chromosome 16 containing Lsamp, a gene which codes for a neuron-associated membrane protein. However, the last region falls in chromosome 7 (115 mbp), a chromosome which contained no LM. This location is downstream of Sox6, a developmental regulator broadly associated with muscle fiber type composition (van Rooij *et al.* 2009), hematopoiesis, bone growth and heart function (Smits *et al.* 2001).

Table 6 Top 5 largest suggestive regions

Chr	Start (BP)	End (BP)	Size	Lowest P
17	17,846,983	23,586,163	5,739,180	7.54E-05
10	103,429,623	105,529,701	2,100,078	3.73E-05
16	31,440,034	33,128,268	1,688,234	7.05E-06
15	18,958,730	20,635,226	1,676,496	8.49E-05
16	16,235,542	17,805,005	1,569,463	7.04E-04

SNPs Fixed in One Treatment and Polymorphic in the Other

SNPs that were fixed in all HR lines and polymorphic in all C lines (FixedHR/PolyC) were grouped into 95 regions, based on their being separated by at least 100 kbp (Table S2). Here, we were more strict on the definition of a group than for the haplotype groups (1 mbp) to limit the

potential for single SNPs to greatly expand the size of a group by their spacing, whereas haplotypes, being made up of several SNPs, are naturally resilient to such inflation. Some of these regions are probably not independently segregating (e.g. chr17: 17,895,909-22,546,405 bp) and might therefore be combined further. Regions varied in size from 1 to 1,626,783 bp. These regions include or are proximal to (in the case of 1 bp regions) 135 transcribed regions, including genes, miRNA, and predicted genes. SNPs that were fixed in all C lines and polymorphic in all HR lines (FixedC/PolyHR) were combined into 64 regions. The size of each region varies from 1 to 753,066 bp. We expect the 1 bp loci may be spurious but chose to include them in results for completeness, especially given that the mini-muscle locus involves only a single base pair (Kelly *et al.* 2013). These regions include or are proximal to 63 transcribed regions, again including genes, miRNA, and predicted genes. FixedHR/PolyC regions were also identified in haplotypes. These haplotype blocks overlapped with the SNP regions identified by FixedHR/PolyC; however, some of the single unlinked loci that met these criteria were not identified using haplotypes.

Ontology Analyses

General Ontology

GO analysis of biological process for the haplotype data reveal "sensory perception of chemical stimulus" to be a major term of interest (Table 7). This appears to be caused by various clusters of olfactory and vomeronasal genes. Many of the most prominent terms appear to be correlated to these olfactory and vomeronasal gene clusters. Although a single, large group of closely linked olfactory genes may overrepresent olfactory's role in selection, we were able to identify two distinct genomic regions of vomeronasal genes and three such regions of olfactory

genes.

The biological process GO terms for LM include many results that are consistent with our previous findings involving the HR mice, including cardiac and myoblast related terms (Table 8). Regulation of locomotion is among the most statistically significant GO terms.

The FixedHR/PolyC GO analyses indicate terms: complement receptor mediated signaling pathway and response to pheromone. These terms were significant with a false discovery rate correction (FDR<0.05), p=7.11E-04 and p=2.40E-07, respectively) (Table 9). For FixedC/PolyHR, no GO terms were significantly enriched with FDR correction, some novel GO terms were deemed most significant. Included in these results is also CDP-choline pathway, which had also been implicated in the haplotype data. The full list of regions for both FixedHR/PolyC and FixedC/PolyHR can be found in (Table S2).

500 **Table 7 Top Biological process terms from GO analysis for Haplotype**

GO Term	Total Genes	Input Genes	Expected	Fold Enrichment	Raw P-Value
detection of chemical stimulus involved in sensory perception of smell	3	1	0.02	47.88	2.74E-02
sensory perception of smell	1,128	27	7.85	3.44	2.46E-08
sensory perception of chemical stimulus	1,228	34	8.55	3.98	5.71E-12
sensory perception	1,641	36	11.42	3.15	7.12E-10
detection of chemical stimulus involved in sensory perception	59	7	0.41	17.04	3.65E-07
detection of stimulus involved in sensory perception	136	8	0.95	8.45	7.40E-06
detection of stimulus	236	9	1.64	5.48	5.40E-05
detection of chemical stimulus	85	7	0.59	11.83	3.53E-06
G protein-coupled receptor signaling pathway	1,853	37	12.9	2.87	4.86E-09
regulation of systemic arterial blood pressure by aortic arch baroreceptor feedback	1	1	0.01	> 100	1.38E-02
system process	2,594	42	18.06	2.33	2.12E-07
multicellular organismal process	7,307	74	50.87	1.45	1.43E-04
nervous system process	2,085	39	14.51	2.69	9.97E-09
sensory perception of sour taste	5	1	0.03	28.73	4.08E-02
sensory perception of taste	71	7	0.49	14.16	1.15E-06
detection of chemical stimulus involved in sensory perception of bitter taste	47	6	0.33	18.34	1.74E-06
sensory perception of bitter taste	51	6	0.36	16.9	2.69E-06
detection of chemical stimulus involved in sensory perception of taste	51	6	0.36	16.9	2.69E-06

501

502 **Table 8 Top biological process terms from GO analysis for LM**

GO Term	Total Genes	Input Genes	Expected	Fold Enrichment	Raw P-Value
locomotory exploration behavior	16	1	0.02	53.6	1.96E-02
locomotory behavior	240	4	0.28	14.29	1.72E-04
behavior	685	6	0.8	7.51	1.17E-04
positive regulation by host of viral release from host cell	5	1	0.01	> 100	6.97E-03
positive regulation of viral release from host cell	15	1	0.02	57.17	1.85E-02
regulation of viral release from host cell	31	1	0.04	27.66	3.66E-02
regulation of locomotion	1040	7	1.21	5.77	1.47E-04
negative regulation of cardiac muscle cell proliferation	17	2	0.02	> 100	2.20E-04
negative regulation of cell population proliferation	684	3	0.8	3.76	4.46E-02
negative regulation of cardiac muscle tissue growth	29	2	0.03	59.14	5.94E-04
regulation of cardiac muscle tissue growth	74	2	0.09	23.18	3.53E-03
regulation of cardiac muscle tissue development	98	2	0.11	17.5	6.02E-03
regulation of striated muscle tissue development	160	2	0.19	10.72	1.52E-02
regulation of muscle tissue development	163	2	0.19	10.52	1.57E-02
regulation of muscle organ development	164	2	0.19	10.46	1.59E-02
regulation of heart growth	80	2	0.09	21.44	4.09E-03
regulation of organ growth	114	2	0.13	15.04	8.02E-03
negative regulation of cardiac muscle tissue development	40	2	0.05	42.88	1.09E-03
negative regulation of striated muscle tissue development	64	2	0.07	26.8	2.67E-03
negative regulation of muscle organ development	66	2	0.08	25.99	2.83E-03
negative regulation of muscle tissue development	67	2	0.08	25.6	2.92E-03
negative regulation of heart growth	29	2	0.03	59.14	5.94E-04
bundle of His cell-Purkinje myocyte adhesion involved in cell communication	6	1	0.01	> 100	8.13E-03
bundle of His cell to Purkinje myocyte communication	13	1	0.02	65.96	1.62E-02
cell communication involved in cardiac conduction	32	1	0.04	26.8	3.78E-02

multicellular organismal signaling	109	2	0.13	15.73	7.37E-03
cardiac muscle cell-cardiac muscle cell adhesion	7	1	0.01	> 100	9.28E-03
cell-cell adhesion	389	3	0.45	6.61	1.04E-02
cell adhesion	789	6	0.92	6.52	2.50E-04
biological adhesion	799	6	0.93	6.44	2.68E-04
negative regulation of cellular extravasation	8	1	0.01	> 100	1.04E-02
negative regulation of leukocyte migration	41	2	0.05	41.83	1.14E-03
regulation of leukocyte migration	209	2	0.24	8.21	2.49E-02
regulation of cell migration	912	5	1.06	4.7	3.71E-03
regulation of cell motility	963	5	1.12	4.45	4.67E-03
negative regulation of cell migration	276	4	0.32	12.43	2.91E-04
negative regulation of cell motility	289	4	0.34	11.87	3.46E-04
negative regulation of cellular component movement	323	4	0.38	10.62	5.24E-04
definitive hemopoiesis	21	2	0.02	81.67	3.25E-04

506 **Table 9 Top GO results for FixedHR/PolyC implicated genes**

GO Term	Total Genes	Input Genes	Expected	Fold Enrichment	Raw P-value
response to pheromone	104	8	0.63	12.7	3.93E-07
complement receptor mediated signaling pathway	13	4	0.08	50.82	2.81E-06
phospholipase C-activating G protein-coupled receptor signaling pathway	91	5	0.55	9.07	2.89E-04
exocytic insertion of neurotransmitter receptor to postsynaptic membrane	8	3	0.05	61.93	3.40E-05
regulation of postsynaptic membrane neurotransmitter receptor levels	62	3	0.38	7.99	7.09E-03
neurotransmitter receptor transport to postsynaptic membrane	20	3	0.12	24.77	3.46E-04
neurotransmitter receptor transport to plasma membrane	21	3	0.13	23.59	3.93E-04
vesicle-mediated transport to the plasma membrane	90	3	0.54	5.51	1.87E-02
neurotransmitter receptor transport	40	3	0.24	12.39	2.21E-03
establishment of protein localization to postsynaptic membrane	21	3	0.13	23.59	3.93E-04
protein localization to postsynaptic membrane	44	3	0.27	11.26	2.85E-03
protein localization to synapse	76	3	0.46	6.52	1.21E-02
receptor localization to synapse	51	3	0.31	9.72	4.23E-03
calcium ion import across plasma membrane	9	2	0.05	36.7	1.91E-03
calcium ion import into cytosol	10	2	0.06	33.03	2.28E-03
calcium ion transport into cytosol	69	3	0.42	7.18	9.40E-03
positive regulation of cytosolic calcium ion concentration	292	7	1.77	3.96	2.26E-03
regulation of cytosolic calcium ion concentration	340	8	2.06	3.89	1.25E-03
cellular calcium ion homeostasis	446	10	2.7	3.7	4.48E-04
calcium ion homeostasis	463	10	2.8	3.57	5.95E-04

507
508
509

Targeted Ontology

The gene search for specific ontologies produced 45-820 genes and 7,315-143,507 SNPs associated with each search (Table 10). The top ten genes were chosen based on the most significant SNP within the gene (Table S4). The most significantly differentiated SNPs were generally found in genes associated with the brain, followed by bone and muscle related genes. Surprisingly, the reward-related ontologies (dopamine and serotonin) did not contain as strong evidence for differentiation as the others.

Table 10 Summary of ontology search.

Search Term	Total Genes	Total SNPs	Top Genes	Top P-value
Dopamin*	254	43,890	*Gnb1, Fpr*[a]*, Adora2a*	1.33E-04
Serotonin	45	7,315	*Htr7, Chrm2, Btbd9*	9.33E-03
Osteo*	491	56,091	*Noct, Nf1, Mmp14*	3.76E-05
Cardiac	820	143,507	*Myh11, Tbx5, Dlg1*	7.25E-06
"Skeletal Muscle"	295	39,383	*Kel, Foxp1, Nf1*	5.23E-06
Brain	667	123,416	*Sorl1, Gak, Fbxo45*	1.92E-07

Genes are listed from most significant to least significant by SNP with lowest p-value

[a] Includes: *Fpr1, Fpr2, Fpr3, Fpr-rs4* (all closely linked)

Consistent Regions Identified Across Multiple Analyses

The major analyses (LM, haplotype, and FixedHR/PolyC) individually implicate about 80, 24, and 46 differentiated genomic regions, respectively. Combined, 61 unique regions across the genome are indicated, including at least one region on every chromosome. Of these 61 regions, 12 are found in all three analyses (Table 11). These 12 consistent regions span just over 27.4 mbp and include 300 validated and predicted genes. Of the 300 genes, 77 are either olfactory or vomeronasal genes, which are predominantly located in two large regions on chromosomes 14 and 17. Surprisingly, many of these regions do not contain many of the most differentiated SNPs according to the multi-model MIVQUE analyses, but do have at least one

SNP with p≤0.001 by the LM criteria.

Table 11 Genomic regions implicated by LM, haplotype, and FixedHR/PolyC analyses

Chr	First BP	Last BP	Included Genes
5	108,000,623	108,679,807	*Tmed5, Ccdc18, Pigg, Mfsd7a, Gak, Tmem175, Slc26a1*
6	41,584,862	41,918,440	*Trpv5, Trpv6, Ephb6, Kel, Llcfc1, Olfr459*
7	29,603,841	29,697,093	*Catsperg2*
9	41,240,184	42,275,833	*Sorl1, Mir100hg, Mir100, Mir125b-1, Mirlet7a-2, Tbcel*[a]
11	79,724,263	80,090,780	*Atad5, Suz12, Utp6, Crlf3*
11	112,227,183	114,489,018	*BC006965, Sox9*
14	52,072,148	53,779,979	*Olfr*[b]*, Trav*[b]
14	97,645,171	98,679,965	*Dach1*
15	18,960,135	20,609,074	*Cdh10, Gm35496*
15	71,023,429	71,559,595	*Fam135b*
16	31,540,757	33,178,952	*Gm536, Rnf168, Ubxn7, Fbxo45, Tnk2, Tnk2os*
17	17,895,909	22,396,753	*Vmn2r*[b]

[a] Tbcel is most differentiated gene in genome based on median p-value
[b] Several genes in this gene family were represented in this region

DISCUSSION

Variation in Genetic Diversity

For the present sample of 79 mice from generation 61, based on the polymorphic SNPs within each line (Table 2), each of the lines continues to retain approximately 34-48% of the total diversity across all 8 lines. Such a drop in genetic diversity would be expected after 61 generation with ~10 breeding pairs per generation per each line. We found no evidence that HR and C lines had differing levels of genetic diversity, averaged across the whole genome.

Consistent Regions from Multiple Analyses

Many of the identified regions span too many genes to allow ready identification of a candidate. However, a few of the regions contain a limited number of genes for which the reported functions make sense in the context of directional selection for high voluntary wheel-running behavior (from first principles of physiology and neurobiology) and/or given previously identified differences between the HR and C lines (see Introduction). Given the rich phenotyping literature on the HR mouse selection experiment (more than 150 publications), we discuss a relatively large number of genes. Additional regions are covered in supplemental material (File S9).

The region identified on chromosome 5 includes 16 genes (excluding predicted and non-coding), three of which were previously identified as differentially expressed in the striatum of the HR and C mice (Saul *et al.* 2017). These genes include *Tmed5, Gak,* and *Mfsd7a*. *Tmed5* is a trafficking protein associated with cell proliferation and WNT7B expression in HeLa cells (Yang *et al.* 2019). Mice knockouts in Gak are generally lethal to adult and developing mice causing various abnormal symptoms, including altered brain development (Lee *et al.* 2008). *Mfsd7a*

(aka *Slc49a3*) has been associated with ovarian cancer, but much remains unknown about this gene (Khan and Quigley 2013).

The region on chromosome 6 includes *Trpv5* and *Kel*, both of which are associated with KO phenotypes that may be tied to known differences between the HR and C lines. Trpv5 KO is associated with phenotypes related to structural changes in the femur and kidney physiology (Hoenderop *et al.* 2003; Loh *et al.* 2013), both of which differ between HR and C lines (Swallow *et al.* 2005; Castro and Garland 2018). *Trpv5* is also associated with calcium homeostasis (Hoenderop *et al.* 2003; Loh *et al.* 2013). Kel is a blood group antigen with KO phenotypes affiliated with weakness, gait and motor coordination, neurological development, and heart function (Zhu *et al.* 2009, 2014). Previous experiments have shown the HR and C mice to have differences in heart physiology (Kolb *et al.* 2013a), gait and motor coordination (Claghorn *et al.* 2017), and brain development (Kolb *et al.* 2013b).

The region on chromosome 9 contains various predicted genes and miRNA, but also one large gene of interest, *Sorl1* (aka *SorlA*). This gene is also implicated in our targeted search for genes related to the brain (Table 10). *Sorl1* codes for a sorting receptor that has been associated with various neural and metabolic diseases (Schmidt *et al.* 2017). Although some of the associated phenotypes, such as obesity, may have some correlation to phenotypic differences between HR and C mice, such as difference in body fat (Swallow *et al.* 2001; Vaanholt *et al.* 2008; Hiramatsu and Garland 2018), this does not directly answer the question of how *Sorl1* influences running behavior. Mouse knockouts in this gene have not shown changes in running gait (Rohe 2008), whereas differences in gait do exist between HR and C mice (Claghorn *et al.* 2017). However, these treadmill tests do not address exercise motivation,

580 which might be influenced by such a neurobiologically relevant gene. Additionally, a more
581 significantly differentiated haplotype can be found over 150,000 bp downstream of *Sorl1*,
582 containing various predicted genes and miRNA. Therefore, further studies will be required to
583 determine precisely the elements of this region that modulate wheel running. Although *Tbcel* is
584 near this consistent region rather than included in it, it is the most differentiated gene in the
585 genome (based on median p-value of included SNPs, p= 4.01E-07). This gene is known to
586 regulate tubulin activity in sperm and the nervous system (Nuwal *et al.* 2012; Frédéric *et al.*
587 2013).

588 One region on chromosome 11 contains numerous genes of potential interest. One LM
589 within this region is proximal to a handful of genes that may be influencing the HR phenotype,
590 including: *Tefm*, *Adap2*, *Crlf3*, and *Suz12*. These genes are associated with KO phenotypes
591 including enlarged heart and decreased body weight (Jiang *et al.* 2019), blood cell
592 concentration (White *et al.* 2013), and brain morphology (Miro *et al.* 2009). All of these
593 phenotypes have been found to differ between HR and C mice (Kolb *et al.* 2013b; Thompson
594 2017; Singleton and Garland 2019).

595 One region on chromosome 14 includes almost exclusively *Dach1*, which is an important
596 regulator for various early developmental genes. *Dach1* is a regulator of muscle satellite cell
597 proliferation and differentiation (Pallafacchina *et al.* 2010). Although knockouts of *Dach1* in
598 mice do not appear to disrupt limb development (Davis *et al.* 2001), *Dach1* mutants sometimes
599 have stunted leg development in *Drosophila* (Mardon *et al.* 1994). Furthermore, *Dach1* has
600 been shown to localize around limb budding regions and interact with known limb patterning
601 genes in both mice and poultry (Horner *et al.* 2002; Kida 2004; Salsi *et al.* 2008). Studies of

skeletal muscle (Garland *et al.* 2002; Bilodeau *et al.* 2009) and of the peripheral skeleton show several differences between HR and C lines of mice (Garland and Freeman 2005; Kelly *et al.* 2006; Castro and Garland 2018; Schwartz *et al.* 2018). This gene has also been implicated in the development and function of the kidneys (Köttgen *et al.* 2010), which have been shown to be larger in the HR lines than C lines in some studies (Swallow *et al.* 2005).

A region on chromosome 15 includes *Cdh10* among a few predicted genes. GO links *Cdh10* to both "calcium ion binding" and "glutamatergic synapse," terms that occasionally produced suggestive p-values for enrichment searches in our differentiation analyses (Table 7, Table 9). These terms could have various implications for the HR mice. *Cdh10* specifically is a cadherin with extensive expression in the brain (Liu *et al.* 2006; Matsunaga *et al.* 2015). This gene has been shown to have increased expression in phrenic neurons (Machado *et al.* 2014), potentially modulating diaphragm movement, and increased functionality of the diaphragm could partly underlie the elevated maximal rate of oxygen consumption during exercise (VO_2max) observed in HR lines (Kolb *et al.* 2010; Hiramatsu *et al.* 2017; Singleton and Garland 2019). *Cdh10* is also known to have increased expression of genes associated with olfactory system development (Akins *et al.* 2007), which could be corroborated by the other two consistent regions associated with olfactory and vomeronasal (see Results, General Ontology). The other region detected on chromosome 15 currently only contains *Fam135b* among its annotations. Few studies have been conducted involving the function of *Fam135b*, but evidence indicates it has an important role in spinal motor neurons based on a > 10,000-fold decrease in expression in spinal and bulbar muscular atrophy models (Sheila *et al.* 2019).

The region we identified on chromosome 16 contains various genes that may influence

wheel running behavior. One example is *Fbxo45*, which has demonstrated itself essential for neuronal development (Saiga *et al.* 2009) and synaptic transmission (Tada *et al.* 2010). One gene that particularly caught our attention was *Pcyt1a*, which is an important modulator of the CDP-choline pathway, catalyzing the formation of CDP-choline (Andrejeva *et al.* 2020), also known as citicoline. Citicoline has been researched extensively for its clinical applications and has demonstrated capacity to stimulate dopamine synthesis in nigrostriatal areas (Drago et al. 1989, cited in Secades and Lorenzo 2006), which are important for exercise and reward (Wise 2009). Additionally, CDP-choline has shown evidence of modulating dopamine receptors in the striatum (Giménez *et al.* 1991).

Ontology

General Ontology

The GO analyses in this paper serve two functions. The first includes determining pathways that have been influenced by the selective breeding protocol. Additionally, the vast publications and data on various morphological and physiological differences between the HR and C lines provide insight into differentiated biological processes.

The Haplotype and Fixed/Poly methods of identifying differentiated genes had considerable overlap between genes and regions identified, which seems to result in similar GO terms for these analyses. The term "sensory perception of chemical stimulus" is expected, given the large number olfactory and vomeronasal genes present in some of these regions. Selection for such genes is likely in response to how the mice are tested for wheel running. For logistical reasons, approximately 2/3 of the mice tested in a given generation were measured on wheels that had not been washed since the previous mouse was on that same wheel,

646 although the attached cages were fresh (Dewan *et al.* 2019). The scent of the previous mouse
647 would potentially elicit different running behavior, dependent on these vomeronasal and
648 olfactory genes (e.g., see Drickamer and Evans 1996). We checked the Allen Brain Atlas for
649 some of these genes (particularly those in the consistent region on chromosome 17) and found
650 that only a few of these olfactory and vomeronasal genes had data. One of these includes
651 *Vmn2r107*, with expression most consistent around the olfactory bulb. However, *Olfr1509* had
652 expression levels seemingly around the anterior cingulate cortex, a region associated with
653 cognitive control of motor behavior (Holroyd *et al.* 2004). GO terms related to postsynaptic
654 neurotransmitters were largely indicated by three genes. *Cplx1* has been linked to severe
655 ataxia and movement limitations in knockout rats (Xu *et al.* 2020), *Dlg1* (aka SAP97) is a
656 scaffolding protein that localizes glutamate receptors in postsynaptic membranes and has
657 shown altered expression in rats exposed to cocaine (Caffino *et al.* 2018), and *Shisa6* has been
658 associated with the localization of AMPA (α-amino-3-hydroxy-5-methyl-4-isoxazolepropionic
659 acid) receptors (Klaassen *et al.* 2016), which have shown reduced expression after prolonged
660 cocaine exposure (Cooper *et al.* 2017). Such terms are perhaps not surprising, given
661 observations of the HR mice having larger midbrains and altered reward mechanisms (Belke
662 and Garland 2007; Mathes *et al.* 2010; Garland *et al.* 2011b; Keeney *et al.* 2012; Kolb *et al.*
663 2013b; Thompson *et al.* 2017).

664 The local maxima GO results are generally quite different from the haplotype and
665 Fixed/Poly analyses. This is partially attributable to less overlapping of identified genomic
666 regions. Additionally, LM is useful for gene culling to reduce influence of hitchhiking genes in
667 the GO analyses. Many of the top terms for LM genes are associated with heart development

668 and function. Heart ventricle mass is greater in the HR mice (Kolb *et al.* 2013a; Kelly *et al.* 2017;
669 Kay *et al.* 2019) and correlates with VO_2max in both HR and C mice (Rezende *et al.* 2006). The
670 genes most associated with cardiac development include *Pkp2*, *Myh11*, and *Tbx5* (also a
671 forelimb regulator). Forelimb development may be altered in the HR mice, while humerus sizes
672 do not seem to differ (Copes *et al.* 2018), differences have been found in metatarsal and
673 metacarpal lengths (Young *et al.* 2009).

674 ## Targeted Ontology

675 As the target ontologies were chosen based on structures and systems known to have been
676 altered by the selective breeding regimen, we would expect to find at least one gene of each
677 ontology that would contain a differentiated SNP. Of these ontologies, "serotonin" and
678 "dopamine" are associated with some of our less impressive p-values (Table 10), with many of
679 the top dopamine-related genes (*Fpr1*, *Fpr2*, *Fpr3*, and *Fpr-rs4*) being present potentially
680 because of linkage to highly differentiated vomeronasal genes (Table 10). However, expression
681 data from the Allen Brain Atlas implicates the *Fpr-rs3* gene as being highly expressed in nucleus
682 raphe obscurus. The nucleus raphe structure is well established for modulating serotonin
683 (Walker and Tadi 2020) and the obscurus region itself has been implicated in modulating
684 respiratory neurons (Lalley *et al.* 1997). As *Fpr-rs3* is the most differentiated gene of the FPR
685 family (median p=0.000393 over 6 SNPs), it may be contributing to the selection signature of
686 this genomic region rather than simply hitchhiking. The most significantly differentiated loci in
687 a dopamine-related gene are in *Gnb1*, part of the Gβγ complex, which activates Girk2 in
688 dopamine neuron membranes (Wang *et al.* 2016). We are surprised not to have found more
689 impressive results for dopamine-related genes, given clear differences in dopamine function

690 between the HR and C mice (Rhodes *et al.* 2001, 2005; Rhodes and Garland 2003; Bronikowski
691 *et al.* 2004; Mathes *et al.* 2010). A possible explanation for this is that trans-regulating sites for
692 these genes have been more influenced by the HR selection regime (Kelly *et al.* 2012; Nica and
693 Dermitzakis 2013). Unfortunately, a limitation of the current study is it lacks the necessary
694 expression data to identify trans-regulating SNPs (Kelly *et al.* 2012, 2014).
695 The remaining ontologies (bone, cardiac, skeletal muscle, and brain) all have at least one
696 gene containing a SNP with p <0.0001 (Table 10). Some of these are included with our LM
697 genes, such as *Myh11* (a myosin gene affiliated with the "cardiac" tag) and *Sorl1* ("Brain" tag).
698 However, some of these are not present among the LM list. Kel, described above as influencing
699 various phenotypes relevant for high running behavior, may appear to be a confusing "miss" for
700 the LM detection process, with a p-value = 1.49E-05. However, the region does have two local
701 maxima, neither of which land in genes, but one is about 15,000 bp upstream of *Kel*. This might
702 be taken as evidence that the LM approach to determining affected genes ought to be modified
703 to better catch nearby genes that could be affected.
704 The expression patterns of the top genes implicated by the "brain" targeted ontology
705 were determined using the Allen Brain Atlas. The top 4 genes (*Sorl1*, *Gak*, *Fbxo45*, and *Tbx3*)
706 showed interesting consistency in their expression patterns. *Sorl1*, *Gak*, and *Fbxo45* all have
707 increased expression around the hippocampus, which has been associate with spatial learning
708 (Schiller *et al.* 2015) and may play a role in addiction (Koob and Volkow 2010). *Sorl1*, *Gak*, and
709 *Tbx3* have higher expression in the retrospenial area, which has also been suggested as a
710 potential modulator of spatial memory (Vann *et al.* 2009), potentially in coordination with the
711 hippocampus (Schiller *et al.* 2015). *Gak* and *Tbx3* both have notable expression levels in the

712 retrohippocampal region, particularly the entorhinal cortex, which is thought to modulate
713 movement speed (Geisler *et al.* 2007; Kropff *et al.* 2015; Ye *et al.* 2018). Additionally, *Gak*,
714 *Fbxo45*, and *Tbx3* have high expression in olfactory regions.

715 The hippocampus has been linked to the regulation of speed during locomotor behavior
716 in both mice and rats by theta (Li *et al.* 2012; Fuhrmann *et al.* 2015; Sheremet *et al.* 2019),
717 gamma (Chen *et al.* 2011; Ahmed and Mehta 2012), and delta oscillations (Furtunato *et al.*
718 2020). Notably, the difference in daily running distance between HR and control lines is
719 attributable mainly to an increase in average (and maximum) running speed, rather than the
720 duration of running, especially in females (e.g., see Garland *et al.* 2011a; Claghorn *et al.* 2016,
721 2017; Copes *et al.* 2018; Hiramatsu and Garland 2018). Another consideration is the impact of
722 physical activity on neurogenesis in the hippocampus (Rhodes *et al.* 2003b; Clark *et al.* 2010;
723 Rendeiro and Rhodes 2018), which, perhaps, could create a sort of feedback loop relating to
724 running speed.

725 ## Comparison with Previous Studies

726 Exercise behavior and the genetic factors that affect it have been the subject of various other
727 GWA and gene expression studies in mice, as well as comparisons of inbred strains (Reviews in
728 Kostrzewa and Kas 2014; Lightfoot *et al.* 2018). In general, these previous studies do not show
729 strong agreement with each other. The primary exception is that several studies have
730 implicated dopamine pathway genes (Bronikowski *et al.* 2004; Lightfoot 2011; Dawes *et al.*
731 2014; Roberts *et al.* 2017). This is of little surprise, as dopamine has been long recognized as a
732 primary neurotransmitter involved with physical activity (Freed and Yamamoto 1985; Rhodes *et*
733 *al.* 2005). As another example of consistencies across previous studies, Dawes et al. (2014)

found differential gene expression in C57L/J (high running) and C3H/HeJ (low running) inbred strains for *Mstn*, a gene previously implicated by Lightfoot et al. (2010) using 41 inbred strains of mice to associate alleles with wheel running. *Mstn* is established as a regulator of skeletal muscle proliferation (Grobet *et al.* 1997; Amthor *et al.* 2007; Mosher *et al.* 2007). The present study contributes several new regions that have not been previously identified (see above). However, we can also identify examples of overlapping results.

We first compiled a list of genes from our study that contain at least one variable SNP (see Materials and Methods). For each gene, all of the SNPs within the transcribed or promotor region were accumulated and the lowest p-value and median p-value (from supplemental File S4) were recorded. These are presented in supplemental File S11. We then cross-reference these p-values (with emphasis on median p-value) against the regions and genes identified by previous studies. This method is limited by not addressing regulatory loci located outside the promotor and transcribed region. For the previous studies, we focused on regions, SNPs, and genes that were specifically associated with running distance, rather than speed or duration of running (if reported), as the HR mice were specifically bred for running distance.

Shimomura et al. (2001) performed an F2 cross between BALB/cJ and C57BL/6J and mapped daily running levels in constant darkness. Although the primary purpose of their study was to identify circadian QTL, two regions were associated directly with wheel-running distance. One of these regions is on chromosome 16 (97,608,543-97,608,688 bp, mm10), not far from one of our local maxima (96,795,226 bp, p=4.97E-04).

A study involving a cross between high- and low-running inbred strains located several markers on both chromosome 9 and chromosome 13 (Lightfoot *et al.* 2008). Although none of

these markers fall within our own significant region on chromosome 9 (about 41,000,000 to 42,000,000 bp), one of the markers identified by Lightfoot et al. (2008) on chromosome 9 is only about 500,000 bp from the gene *Leo1*. For our sample of mice, only one SNP in this gene was polymorphic, and it was in the non-coding region (File S11: p=0.00186)

Lightfoot et al. (2010) used haplotype association mapping to identify 12 QTL associated with wheel running among 41 inbred strains of mice. One of the regions they identified on chromosome 5 (114,584,508-117,669,848 bp after conversion to mm10) is intriguingly close to one of our own haplotype regions (118,824,587-119,299,787 bp, Table 5). Additionally, we detected a local maximum on chromosome 12 (88,919,735 bp, p=7.54E-05) near their identified haplotype (88,113,842-88,220,086 bp, mm10). Lightfoot et al. (2010) also identified a region on chromosome 13 (95,477,271-95,863,515 bp, mm10), which coincides with a few of our FixedHR/PolyC loci (95,595,237-95,947,205 bp). Aside from these, the best example of similarity with the present study is a gene on chromosome 8 (*Galntl6*) that was found as suggestive in the current study (File S11, median p=0.039, SNPs=5,925). Lightfoot et al. (2010) also identified a region on chromosome 12, about 0.5 mbp upstream of *Nrxn3*. Both our LM and FixedHR/PolyC methods indicated this gene as a strong candidate, with a segment of intron 1 containing several low p-values (median p=2.04E-04, SNPs=195), but it was not listed as a consistent region because the haplotype results did not produce a significant haplotype near *Nrxn3*. *Nrxn3* is a single-pass transmembrane protein found in presynaptic terminals and functions as a cell adhesion molecule (Stoltenberg *et al.* 2011; Kasem *et al.* 2018). *Nrxn3* creates particular interest in that it is associated with various addictive behaviors (Zheng *et al.* 2018), which is consistent with evidence that the HR mice are to some extent addicted to

778 running (Rhodes *et al.* 2005; Kolb *et al.* 2013b). Previous work has associated *Nrxn3* with
779 addictive behaviors involving nicotine (Wolock *et al.* 2013) and opioids (Lachman *et al.* 2007),
780 predominantly through association and expression studies (Kasem *et al.* 2018). Exercise
781 addiction is not a new concept, but remains controversial (Nogueira *et al.* 2018).
782 QTL mapping of the G_4 intercross of C57BL/6J with one of the four HR lines implicated a
783 region on chromosome 7 (101 – 130 mbp) that contains numerous olfactory/vomeronasal
784 genes (Kelly *et al.* 2010). We identified FixedHR/PolyC SNPs within that region at 127,385,309 -
785 127,947,542 bp. We also identified vomeronasal genes on chromosome 17. (Kelly et al. [2010]
786 reported other QTL associated with running on the first two days of wheel exposure, but this
787 phenotype may reflect variation in neophobia more than exercise motivation or ability.)
788 Saul et al. (2017) performed expression analysis using the striatum of the HR and C lines
789 from generation 66. The mice were sampled after several hours of wheel deprivation, which is
790 believed to induce high expression of motivation-related genes (Rhodes *et al.* 2003a). Some of
791 their highlighted differentially expressed genes include: *Htr1b*, *Slc38a2*, *Tmed5*,
792 *5031434O11Rik*, *Gak*, *Mfsd7a*, and *Gpr3*. *Tmed5*, *Gak*, and *Mfsd7a* are all found within a highly
793 differentiated region in our SNP data (median p=4.85E-04 for all three genes, SNPs=671, File
794 S11). Although *5031434O11Rik* and the associated *Setd7* are not found within our consistent
795 regions (due to no FixedHR/PolyC SNPs), they both contain many of the most differentiated loci
796 of individual SNP analyses (median p=3.78E-05, SNPs=4). Knockouts of *Setd7* (aka *Set9*) have
797 been associated with altered lung development and morphology (Elkouris *et al.* 2016). Lung
798 differences in the HR and C lines have not been greatly explored. Three studies have reported
799 no statistical difference in lung mass (Meek *et al.* 2009; Kolb *et al.* 2010; Dlugosz *et al.* 2013),

but an unpublished study of males from generation 21 found that HR lines tended to have higher pulmonary diffusion capacity and capillary surface area determined via morphometry (T. Garland, and S. F. Perry, personal communication), and a study of females from generation 37 reported a trend for HR mice to have higher dry lung mass (Meek *et al.* 2009; Kelly *et al.* 2017). We are uncertain of what *Setd7* may be doing in the brain. However, the Allen Brain Atlas does indicate increased expression levels of *Setd7* in the sensory regions of the midbrain, motor related regions of the medulla, and the cerebellar cortex, which has been associated with motor function and reward (Doya 2000). Furthermore, *Setd7* has been shown to modulate pain and inflammation following nerve injury, potentially enabling an individual to proceed to exercise despite injury (Shen *et al.* 2019).

Overall, studies attempting to identify the genetic underpinnings of exercise behavior in rodents have produced a wide variety of results. We can offer several reasons for such inconsistencies. First, some of these studies address gene expression (Bronikowski *et al.* 2003, 2004; Dawes *et al.* 2014; Saul *et al.* 2017) and eQTL (Kelly *et al.* 2012, 2014), which will commonly implicate different genetic factors for complex traits than studies looking at genetic variants, likely as a result of complex interactions between genetic variants and gene expression (Bouchard 2015; Parker *et al.* 2016). Second, some studies compare inbred strains (Lightfoot *et al.* 2008, 2010; Dawes *et al.* 2014) with very different genetic histories and likely different biologically significant alleles available to them than in the Hsd:ICR mice that formed the basis for the present selection experiment. Furthermore, a trait as complex as voluntary exercise (Lightfoot *et al.* 2018) would be expected to have numerous underlying subordinate traits which, in turn, could have innumerable potential genetic factors modulating them

822 (Garland *et al.* 2016; Sella and Barton 2019). Finally, in the current study, we sought to detect
823 specifically those factors that are shared across all 4 HR lines, which likely does not reflect all of
824 the exercise-relevant loci that vary among the replicate HR lines. However, those alleles
825 implicated by all four HR lines arguably provide the strongest evidence for biologically
826 significant regions in this selection experiment and also for the Hsd:ICR base population.

827 ## Mini-Muscle Allele

828 The mini-muscle phenotype was discovered in the HR selection experiment and is associated
829 with alterations in various organs, especially skeletal muscle, but also including heart, kidney,
830 and overall body mass of the mice (Swallow *et al.* 2005; Meek *et al.* 2009; Kolb *et al.* 2013a;
831 Talmadge *et al.* 2014; Kay *et al.* 2019) as well as behaviors (Kelly *et al.* 2006; Singleton and
832 Garland 2019). This phenotype is caused by a single recessive SNP mutation located in an *Myh4*
833 (myosin heavy polypeptide 4) gene (Kelly *et al.* 2013). Mice expressing the mini-muscle
834 phenotype have often been found to run faster and sometimes for longer distances than other
835 HR mice (Kolb *et al.* 2013a). This polymorphism was lost, presumably via random genetic drift,
836 from all lines except for HR lines 3 (where it went to fixation) and line 6 (where it remains
837 polymorphic with the wildtype allele). Population-genetic analyses indicate that the allele was
838 under positive selection in the HR lines (Garland *et al.* 2002). The current WGS data show
839 (generation 61) that the mutation is still only present in lines 3 (fixed) and 6, with allele
840 frequency of 0.65 in line 6. As the mini-muscle phenotype appears to enable faster overall
841 running on wheels at the cost of running duration, it has been regarded as an alternative
842 "solution" to the selection criterion (Garland *et al.* 2011a), not unlike the concept of "private"
843 alleles (Martin *et al.* 1996). Such a mutation is expected to change the genetic background of

line 3 (and to a lesser extent, line 6) giving rationale to analyzing these lines separately for possible QTL, in future studies.

Allele Frequency Implications

The general pattern of allele frequencies across the replicate lines can be used to infer patterns of selection. Table 12 includes some of the potential profiles that could possibly be observed and (for the most part) were observed in the WGS data.

Profile 1 No observed genetic variation. For our 79 mice, this accounts for about 99.8% of the genome (Table 2).

Profile 2 Fixation for alternate alleles in the two selection treatments would imply opposing directional selection, as might occur in experiments with replicate lines selected for high versus low values of a trait. The HR mouse selection experiment includes high-selected and control treatments, but not a low-selected treatment. Thus, fixation for alternate alleles in the HR and C lines would not necessarily be expected, and indeed was never observed for either the WGS data or the MegaMUGA data reported previously (Xu and Garland 2017). Importantly, even data from selection experiments that include high- and low-selected treatments are not showing much evidence of fixation for alternate alleles (Burke *et al.* 2010; Lillie *et al.* 2019).

Profile 3 Stabilizing selection or random drift for one group and directional selection for the other. This was the focus of the scans for loci fixed in all lines of one linetype and polymorphic in all lines of the other (Fixed/Poly) in our own haplotype and WGS data and produced several prospective regions of interest. The fixed allele can either be entirely the reference (0) or alternative (1).

Profile 4 Selection for test group 2 but evidence of drift for group 1 (likely caused by little to no

selection). Some of the loci of the WGS SNP data meet this profile. For example, Chromosome 11: 96,332,082 bp (p=0.051).

Profile 5 Random genetic drift for both test groups. Such loci will be among those analyzed, but this pattern of differentiation is unlikely to result from the selective breeding regimen.

Table 12 Potential fixation profiles

	Test Group 1				Test Group 2			
Profile	Rep 1	Rep 2	Rep 3	Rep 4	Rep 1	Rep 2	Rep 3	Rep 4
1	0	0	0	0	0	0	0	0
2	0	0	0	0	1	1	1	1
3	Het	Het	Het	Het	0	0	0	0
4	0	0	1	1	0	0	0	0
5	0	0	1	1	0	0	1	1

In general, as with any population that is relatively well adapted to the prevailing environmental conditions, breeding colonies of laboratory house mice maintained under standard vivarium housing conditions should experience continuing stabilizing selection at many loci. Under standard housing conditions, an allele with a strong positive influence on wheel running, or activity in cages without wheels, might be disfavored if it were negatively associated with such aspects of the life history as litter size or maternal care. In contrast, under the conditions of the HR mouse selection experiment, an allele with a strong positive influence on wheel running might be expected to go to fixation rapidly in all HR lines in a manner consistent with a "complete sweep" (Burke 2012). Thus, to fix an allele, directional selection in the HR lines must be strong enough to overcome a presumed prevailing background of stabilizing selection and possibly negative selection. Regions that are FixedHR/PolyC (profile 3) should, therefore, be indicative of relatively strong directional selection in the HR lines.

886 Alternatively, some loci may have come under stabilizing selection in the HR lines, e.g.,
887 due to heterozygote advantage or epistatic interactions with other loci, preventing them from
888 going to fixation. Hence, we also examined loci polymorphic in all HR lines but fixed in all C
889 lines (FixedC/PolyHR). The GO analyses of the included genes in these regions were
890 consistently less significant (raw p≥0.0026 for all implicated terms). However, such terms as
891 "synapse assembly" and those related to glycerolipids emerged may merit further exploration.

892 ## Interpretation of the Four Models

893 The four models in the multi-model analysis were included to allow for different variance
894 structures within and between the HR and C linetypes. The within-line variance is the variability
895 of allele frequency among the ~10 mice within each line. This variance is zero when a line is
896 fixed for one allele or another, but maximized when 5 mice within each line are homozygous for
897 one allele while 5 mice are homozygous for the other. The among-line variance indicates how
898 different the replicate lines within a linetype are from each other. This variance component is
899 minimized when all four lines within a linetype are fixed for the same allele, but maximized
900 when two lines are fixed for one allele while two lines are fixed for the other.

901 In principle, both the within-line and among-line variances can differ between the two
902 selection treatments (linetypes); hence, the Full model includes separate estimates of both
903 within- and among-line variances. For wheel running in later generations of the selection
904 experiment, a full model has been shown to fit well (Garland *et al.* 2011a). The SepVarInd
905 model includes only the within-line variance. The SepVarLine model includes only the among-
906 line variance. Lastly, the Simple model does not include either of these two variances, and
907 corresponds to the single model used by Xu and Garland (2017).

As expected, we found many loci that were better fit by models other than the Simple model used by Xu and Garland (2017) (Table 4). Figure 3 gives examples. In A, the Full model is implemented because C lines exhibit very little within- and among-line variance while HR lines exhibit both. In B, the SepVarInd model is used because C lines have high within-line variance (while HR lines are comparatively low), but both have similar among-line variance. In C, SepVarLines model is used because nearly all lines contain very little within-line variance (6 are fixed for a single allele), but C lines, being fixed for opposing alleles, creates different among-line variance. D identifies a Simple model locus because these variances are roughly the same for the different linetypes. E represents a locus with no within-line variance and thus could not be analyzed with the mixed model ANOVA like other loci. However, use of multiple models did not increase the number of loci identified as statistically significant based on repeat analyses of the MEGAMuga data with both methods (Figure 1).

Figure 3 These are images of different variance structures depicted by actual examples from the MegaMUGA data (Xu and Garland 2017). This includes example data that were best fit by the "Full" model (A), "SepVarInd" model (B), "SepVarLines" model (C), and the "Simple" model (D). E shows a locus that had no within-line variance. P-values are significance levels for comparing the HR and C lines.

A "Full" Model

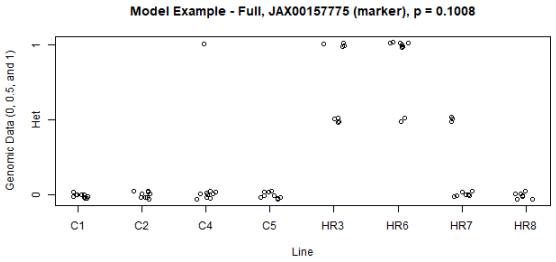

B "SepVarInd" Model

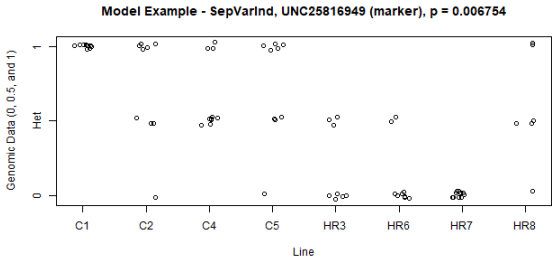

C "SepVarLines" Model

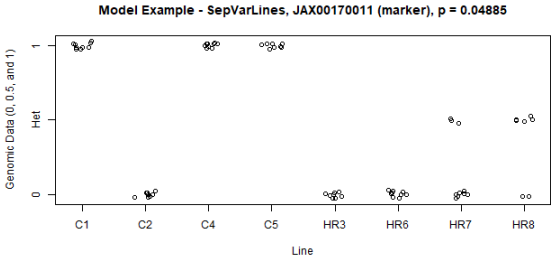

D "Simple" Model

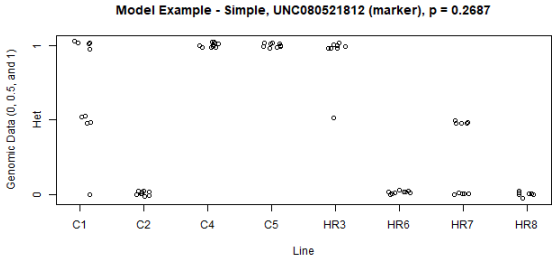

E No Within-line Variance

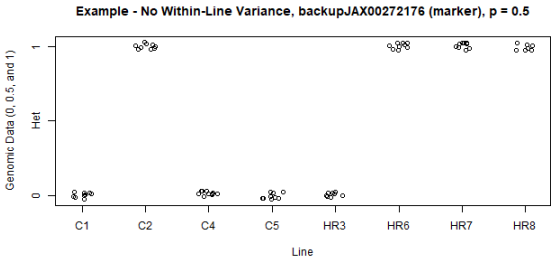

SUMMARY, LIMITATIONS, AND FUTURE DIRECTIONS

Exercise, or the lack of exercise, has far-reaching medical and financial implications (Manley 1996; Booth *et al.* 2012; Carlson *et al.* 2015). Numerous studies have provided strong evidence for the existence of genetic underpinnings of exercise behavior and physical activity (Kostrzewa and Kas 2014; Lightfoot *et al.* 2018), including in the High Runner mouse selection experiment (Bronikowski *et al.* 2003, 2004; Careau *et al.* 2013; Saul *et al.* 2017; Xu and Garland 2017). Here we have used three different analytical methods with whole-genome sequence data to address the genetic basis of the 3-fold increase in daily running distances observed in the four replicate selectively bred HR lines of mice. These methods include haplotype and SNP statistical analysis, as well as non-statistical analysis of fixation patterns in HR and C lines.

The intersection of multiple analyses indicated 61 genomic regions of differentiation, with 12 identified as of particular interest. These regions include genes known to influence systems that have already been demonstrated to differ between HR and Control mice, such as response to conspecific odors, brain development, body weight, and relative heart size. However, they also contain genes whose role in voluntary running behavior is as yet unclear.

This study does have the limitation of focusing on males, whereas exercise behavoir and much of the physiology and morphology related to exercise abilities differ between sexes in both rodents and humans (Eikelboom and Mills 1988; Thomas and Thomas 1988; Rowland 2016; Sheel 2016; Rosenfeld 2017; Thompson *et al.* 2017). A natural next step would then be to conduct similar analyses in females. This approach, however, can establish correlation but not causation. Therefore, studies of wheel-running behavoir of mice with knockouts or Cre modifications of genes in some of the genomic regions identified here may help to establish or

dismiss causal relationships between the genes and phenotype. Furthermore, as the HR mouse experiment has complete pedigree information for all mice and lines (Careau *et al.* 2013, 2015), it will also be possible to use this information to better account for relatedness between mice in statistical analyses and so provide more informed estimates of loci acted upon by selection.

Importantly, none of the analytical approaches we used address the possibility of "private alleles" (Martin *et al.* 1996) in one or more of the HR lines that may influence exercise behavior, thus representing "multiple solutions" to the selective breeding regime (Garland *et al.* 2011a), but this will be an important possibility to consider in future studies. We already know of one private allele of major effect (mini-muscle) that has far-reaching effects on mouse muscle and organ development (Swallow *et al.* 2005; McGillivray *et al.* 2009; Kelly *et al.* 2013), as well as many other aspects of the phenotype, and has been favored by the selection protocol (Garland *et al.* 2002). Determination of such alleles will be an important area for future research.

Acknowledgments

Supported by NSF grant DEB-1655362 to T.G.

Author contributions:

Conceptualization, D.A.H., L.Y., F.P.M.dEV., D.P., S.X., F.C., T.G.; investigation, D.A.H., L.Y., G.M.W., F.P.M.dEV., D.P., A.S.F., F.C., T.G.; software, D.A.H., L.Y., S.X.; formal analysis, D.A.H., L.Y., A.S.F., S.X., F.C., T.G.; writing – original draft, D.A.H., L.Y., A.S.F., F.C., T.G.; writing – review and editing, D.A.H., L.Y., G.M.W., F.P.M.dEV., D.P., A.S.F., S.X., F.C., T.G.

Literature Cited

Aebi, M., M. M. J. van Donkelaar, G. Poelmans, J. K. Buitelaar, E. J. S. Sonuga-Barke *et al.*, 2016 Gene-set and multivariate genome-wide association analysis of oppositional defiant behavior subtypes in attention-deficit/hyperactivity disorder. Am. J. Med. Genet. B Neuropsychiatr. Genet. 171: 573–588.

Ahmed, O. J., and M. R. Mehta, 2012 Running speed alters the frequency of hippocampal gamma oscillations. J. Neurosci. 32: 7373–7383.

Akins, M. R., D. L. Benson, and C. A. Greer, 2007 Cadherin expression in the developing mouse olfactory system. J. Comp. Neurol. 501: 483–497.

Amthor, H., R. Macharia, R. Navarrete, M. Schuelke, S. C. Brown *et al.*, 2007 Lack of myostatin results in excessive muscle growth but impaired force generation. Proc. Natl. Acad. Sci. 104: 1835–1840.

Andrejeva, G., S. Gowan, G. Lin, A.-C. L. Wong Te Fong, E. Shamsaei *et al.*, 2020 *De novo* phosphatidylcholine synthesis is required for autophagosome membrane formation and maintenance during autophagy. Autophagy 16: 1044–1060.

Belke, T. W., and T. Garland, Jr., 2007 A brief opportunity to run does not function as a reinforcer for mice selected for high daily wheel-running rates. J. Exp. Anal. Behav. 88: 199–213.

Benjamin, E. J., P. Muntner, A. Alonso, M. S. Bittencourt, C. W. Callaway *et al.*, 2019 Heart Disease and Stroke Statistics—2019 Update: A Report From the American Heart Association. Circulation 139:.

Bilodeau, G. M., H. Guderley, D. R. Joanisse, and T. Garland, Jr., 2009 Reduction of type IIb myosin and IIB fibers in tibialis anterior muscle of mini-muscle mice from high-activity lines. J. Exp. Zool. Part Ecol. Genet. Physiol. 311A: 189–198.

Blair, S. N., and J. N. Morris, 2009 Healthy Hearts—and the universal benefits of being physically active: physical activity and health. Ann. Epidemiol. 19: 253–256.

1000 Booth, F. W., M. V. Chakravarthy, S. E. Gordon, and E. E. Spangenburg, 2002 Waging war on physical
1001 inactivity: using modern molecular ammunition against an ancient enemy. J. Appl. Physiol. 93:
1002 3–30.
1003 Booth, F. W., C. K. Roberts, and M. J. Laye, 2012 Lack of exercise is a major cause of chronic diseases, in
1004 *Comprehensive Physiology*, edited by R. Terjung. John Wiley & Sons, Inc., Hoboken, NJ, USA.
1005 Bouchard, C., 2015 Exercise genomics—a paradigm shift is needed: a commentary: Table 1. Br. J. Sports
1006 Med. 49: 1492–1496.
1007 Britton, S. L., and L. G. Koch, 2001 Animal genetic models for complex traits of physical capacity: Exerc.
1008 Sport Sci. Rev. 29: 7–14.
1009 Bronikowski, A. M., P. A. Carter, T. J. Morgan, T. Garland, Jr., N. Ung *et al.*, 2003 Lifelong voluntary
1010 exercise in the mouse prevents age-related alterations in gene expression in the heart. Physiol.
1011 Genomics 12: 129–138.
1012 Bronikowski, A. M., J. S. Rhodes, T. Garland, Jr., T. A. Prolla, T. A. Awad *et al.*, 2004 The evolution of gene
1013 expression in mouse hippocampus in response to selective breeding for increased locomotor
1014 activity. Evolution 58: 2079–2086.
1015 Burke, M. K., 2012 How does adaptation sweep through the genome? Insights from long-term selection
1016 experiments. Proc. R. Soc. B Biol. Sci. 279: 5029–5038.
1017 Burke, M. K., J. P. Dunham, P. Shahrestani, K. R. Thornton, M. R. Rose *et al.*, 2010 Genome-wide analysis
1018 of a long-term evolution experiment with *Drosophila*. Nature 467: 587–590.
1019 Caffino, L., G. Messa, and F. Fumagalli, 2018 A single cocaine administration alters dendritic spine
1020 morphology and impairs glutamate receptor synaptic retention in the medial prefrontal cortex
1021 of adolescent rats. Neuropharmacology 140: 209–216.

1022 Careau, V., M. E. Wolak, P. A. Carter, and T. Garland, Jr., 2015 Evolution of the additive genetic variance–
1023 covariance matrix under continuous directional selection on a complex behavioural phenotype.
1024 Proc. R. Soc. B Biol. Sci. 282: 20151119.
1025 Careau, V., M. E. Wolak, P. A. Carter, and T. Garland, Jr., 2013 Limits to behavioral evolution: the
1026 quantative genetics of a complex trait under directional selection. Evolution 67: 3102–3119.
1027 Carlson, S. A., J. E. Fulton, M. Pratt, Z. Yang, and E. K. Adams, 2015 Inadequate physical activity and
1028 health care expenditures in the United States. Prog. Cardiovasc. Dis. 57: 315–323.
1029 Castro, A. A., and T. Garland, Jr., 2018 Evolution of hindlimb bone dimensions and muscle masses in
1030 house mice selectively bred for high voluntary wheel-running behavior. J. Morphol. 279: 766–
1031 779.
1032 Chen, Z., E. Resnik, J. M. McFarland, B. Sakmann, and M. R. Mehta, 2011 Speed controls the amplitude
1033 and timing of the hippocampal gamma rhythm (A. Borst, Ed.). PLoS ONE 6: e21408.
1034 Claghorn, G. C., I. A. T. Fonseca, Z. Thompson, C. Barber, and T. Garland, Jr., 2016 Serotonin-mediated
1035 central fatigue underlies increased endurance capacity in mice from lines selectively bred for
1036 high voluntary wheel running. Physiol. Behav. 161: 145–154.
1037 Claghorn, G. C., Z. Thompson, J. C. Kay, G. Ordonez, T. G. Hampton *et al.*, 2017 Selective breeding and
1038 short-term access to a running wheel alter stride characteristics in house mice. Physiol.
1039 Biochem. Zool. 90: 533–545.
1040 Clark, P. J., R. A. Kohman, D. S. Miller, T. K. Bhattacharya, E. H. Haferkamp *et al.*, 2010 Adult hippocampal
1041 neurogenesis and c-Fos induction during escalation of voluntary wheel running in C57BL/6J
1042 mice. Behav. Brain Res. 213: 246–252.
1043 Cooper, S., A. J. Robison, and M. S. Mazei-Robison, 2017 Reward circuitry in addiction.
1044 Neurotherapeutics 14: 687–697.

1045 Copes, L. E., H. Schutz, E. M. Dlugsoz, S. Judex, and T. Garland, Jr., 2018 Locomotor activity, growth
1046 hormones, and systemic robusticity: An investigation of cranial vault thickness in mouse lines
1047 bred for high endurance running. Am. J. Phys. Anthropol. 166: 442–458.
1048 Cordeiro, L. M. S., P. C. R. Rabelo, M. M. Moraes, F. Teixeira-Coelho, C. C. Coimbra *et al.*, 2017 Physical
1049 exercise-induced fatigue: The role of serotonergic and dopaminergic systems. Braz. J. Med. Biol.
1050 Res. 50:.
1051 Cornelissen, V. A., and R. H. Fagard, 2005 Effects of endurance training on blood pressure, blood
1052 pressure–regulating mechanisms, and cardiovascular risk factors. Hypertension 46: 667–675.
1053 Cornier, M.-A., D. Dabelea, T. L. Hernandez, R. C. Lindstrom, A. J. Steig *et al.*, 2008 The metabolic
1054 syndrome. Endocr. Rev. 29: 777–822.
1055 Davis, R. J., W. Shen, Y. I. Sandler, M. Amoui, P. Purcell *et al.*, 2001 Dach1 mutant mice bear no gross
1056 abnormalities in eye, limb, and brain development and exhibit postnatal lethality. Mol. Cell. Biol.
1057 21: 1484–1490.
1058 Dawes, M., T. Moore-Harrison, A. T. Hamilton, T. Ceaser, K. J. Kochan *et al.*, 2014 Differential gene
1059 expression in high- and low-active inbred mice. BioMed Res. Int. 2014: 1–9.
1060 De Moor, M. H. M., Y.-J. Liu, D. I. Boomsma, J. Li, J. J. Hamilton *et al.*, 2009 Genome-wide association
1061 study of exercise behavior in dutch and american adults: Med. Sci. Sports Exerc. 41: 1887–1895.
1062 Dewan, I., T. Garland, Jr., L. Hiramatsu, and V. Careau, 2019 I smell a mouse: indirect genetic effects on
1063 voluntary wheel-running distance, duration and speed. Behav. Genet. 49: 49–59.
1064 Didion, J. P., A. P. Morgan, L. Yadgary, T. A. Bell, R. C. McMullan *et al.*, 2016 *R2d2* drives selfish sweeps in
1065 the house mouse. Mol. Biol. Evol. 33: 1381–1395.
1066 Dietrich, A., 2004 Endocannabinoids and exercise. Br. J. Sports Med. 38: 536–541.

1067 Dlugosz, E. M., H. Schutz, T. H. Meek, W. Acosta, C. J. Downs *et al.*, 2013 Immune response to a
1068 Trichinella spiralis infection in house mice from lines selectively bred for high voluntary wheel
1069 running. J. Exp. Biol. 216: 4212–4221.
1070 Doya, K., 2000 Complementary roles of basal ganglia and cerebellum in learning and motor control. Curr.
1071 Opin. Neurobiol. 10: 732–739.
1072 Drickamer, L. C., and T. R. Evans, 1996 Chemosignals and activity of wild stock house mice, with a note
1073 on the use of running wheels to assess activity in rodents. Behav. Processes 36: 51–66.
1074 Dyrstad, S. M., B. H. Hansen, I. M. Holme, and S. A. Anderssen, 2014 Comparison of self-reported versus
1075 accelerometer-measured physical activity. Med. Sci. Sports Exerc. 46: 99–106.
1076 Eikelboom, R., and R. Mills, 1988 A microanalysis of wheel running in male and female rats. Physiol.
1077 Behav. 43: 625–630.
1078 Elkouris, M., H. Kontaki, A. Stavropoulos, A. Antonoglou, K. C. Nikolaou *et al.*, 2016 SET9-mediated
1079 regulation of TGF-β signaling links protein methylation to pulmonary fibrosis. Cell Rep. 15: 2733–
1080 2744.
1081 Ernst, C., A. K. Olson, J. P. J. Pinel, R. W. Lam, and B. R. Christie, 2006 Antidepressant effects of exercise:
1082 Evidence for an adult-neurogenesis hypothesis? J Psychiatry Neurosci 31: 84–92.
1083 Fan, W., A. R. Atkins, R. T. Yu, M. Downes, and R. M. Evans, 2013 Road to exercise mimetics: targeting
1084 nuclear receptors in skeletal muscle. J. Mol. Endocrinol. 51: T87–T100.
1085 Fisher, R. A., 1925 Statistical methods for research workers, pp. 25–235 in *Biological monographs and*
1086 *manuals*, edited by F. A. E. Crew and D. W. Cutler. Oliver and Boyd (Edinburgh).
1087 Frédéric, M. Y., V. F. Lundin, M. D. Whiteside, J. G. Cueva, D. K. Tu *et al.*, 2013 Identification of 526
1088 conserved metazoan genetic innovations exposes a new role for cofactor E-like in neuronal
1089 microtubule homeostasis (A. D. Chisholm, Ed.). PLoS Genet. 9: e1003804.

Freed, C., and B. Yamamoto, 1985 Regional brain dopamine metabolism: a marker for the speed, direction, and posture of moving animals. Science 229: 62–65.

Fuhrmann, F., D. Justus, L. Sosulina, H. Kaneko, T. Beutel *et al.*, 2015 Locomotion, theta oscillations, and the speed-correlated firing of hippocampal neurons are controlled by a medial septal glutamatergic circuit. Neuron 86: 1253–1264.

Furtunato, A. M. B., B. Lobão-Soares, A. B. L. Tort, and H. Belchior, 2020 Specific increase of hippocampal delta oscillations across consecutive treadmill runs. Front. Behav. Neurosci. 14:.

Garland, Jr., T., and P. W. Freeman, 2005 Selective breeding for high endurance running increases hindlimb symmetry. Evolution 59: 1851–1854.

Garland, Jr., T., S. A. Kelly, J. L. Malisch, E. M. Kolb, R. M. Hannon *et al.*, 2011a How to run far: multiple solutions and sex-specific responses to selective breeding for high voluntary activity levels. Proc. R. Soc. B Biol. Sci. 278: 574–581.

Garland, Jr., T., M. T. Morgan, J. G. Swallow, J. S. Rhodes, I. Girard *et al.*, 2002 Evolution of a small-muscle polymorphism in lines of house mice selected for high activity levels. Evolution 56: 1267–1275.

Garland, Jr., T., and M. R. Rose, 2009 *Experimental evolution: concepts, methods, and applications of selection experiments*. University of California Press.

Garland, Jr., T., H. Schutz, M. A. Chappell, B. K. Keeney, T. H. Meek *et al.*, 2011b The biological control of voluntary exercise, spontaneous physical activity and daily energy expenditure in relation to obesity: human and rodent perspectives. J. Exp. Biol. 214: 206–229.

Garland, Jr., T., M. Zhao, and W. Saltzman, 2016 Hormones and the evolution of complex traits: insights from artificial selection on behavior. Integr. Comp. Biol. 56: 207–224.

Geisler, C., D. Robbe, M. Zugaro, A. Sirota, and G. Buzsaki, 2007 Hippocampal place cell assemblies are speed-controlled oscillators. Proc. Natl. Acad. Sci. 104: 8149–8154.

Giménez, R., J. Raïch, and J. Aguilar, 1991 Changes in brain striatum dopamine and acetylcholine receptors induced by chronic CDP-choline treatment of aging mice. Br. J. Pharmacol. 104: 575–578.

Grobet, L., L. J. Royo Martin, D. Poncelet, D. Pirottin, B. Brouwers *et al.*, 1997 A deletion in the bovine myostatin gene causes the double–muscled phenotype in cattle. Nat. Genet. 17: 71–74.

Guthold, R., G. A. Stevens, L. M. Riley, and F. C. Bull, 2018 Worldwide trends in insufficient physical activity from 2001 to 2016: a pooled analysis of 358 population-based surveys with 1·9 million participants. Lancet Glob. Health 6: e1077–e1086.

Herbert, A. J., A. G. Williams, P. J. Hennis, R. M. Erskine, C. Sale *et al.*, 2019 The interactions of physical activity, exercise and genetics and their associations with bone mineral density: implications for injury risk in elite athletes. Eur. J. Appl. Physiol. 119: 29–47.

Hiramatsu, L., and T. Garland, Jr., 2018 Mice selectively bred for high voluntary wheel-running behavior conserve more fat despite increased exercise. Physiol. Behav. 194: 1–8.

Hiramatsu, L., J. C. Kay, Z. Thompson, J. M. Singleton, G. C. Claghorn *et al.*, 2017 Maternal exposure to Western diet affects adult body composition and voluntary wheel running in a genotype-specific manner in mice. Physiol. Behav. 179: 235–245.

Hoenderop, J. G. J., J. P. T. M. van Leeuwen, B. C. J. van der Eerden, F. F. J. Kersten, A. W. C. M. van derKemp *et al.*, 2003 Renal Ca2+ wasting, hyperabsorption, and reduced bone thickness in mice lacking TRPV5. J. Clin. Invest. 112: 1906–1914.

Holroyd, C., S. Nieuwenhuis, R. Mars, and M. Coles, 2004 Anterior cingulate cortex, selection for action, and error processing, pp. 219–31 in *Cognitive neuroscience of attention*, Guilford Press, New York.

Horner, A., L. Shum, J. A. Ayres, K. Nonaka, and G. H. Nuckolls, 2002 Fibroblast growth factor signaling regulates Dach1 expression during skeletal development. Dev. Dyn. 225: 35–45.

Horwitz, T., K. Lam, Y. Chen, Y. Xia, and C. Liu, 2019 A decade in psychiatric GWAS research. Mol. Psychiatry 24: 378–389.

Jiang, S., C. Koolmeister, J. Misic, S. Siira, I. Kühl *et al.*, 2019 TEFM regulates both transcription elongation and RNA processing in mitochondria. EMBO Rep. 20:.

Kasem, E., T. Kurihara, and K. Tabuchi, 2018 Neurexins and neuropsychiatric disorders. Neurosci. Res. 127: 53–60.

Kay, J. C., G. C. Claghorn, Z. Thompson, T. G. Hampton, and T. Garland, Jr., 2019 Electrocardiograms of mice selectively bred for high levels of voluntary exercise: Effects of short-term exercise training and the mini-muscle phenotype. Physiol. Behav. 199: 322–332.

Keeney, B. K., T. H. Meek, K. M. Middleton, L. F. Holness, and T. Garland, Jr., 2012 Sex differences in cannabinoid receptor-1 (CB1) pharmacology in mice selectively bred for high voluntary wheel-running behavior. Pharmacol. Biochem. Behav. 101: 528–537.

Kelly, S. A., T. A. Bell, S. R. Selitsky, R. J. Buus, K. Hua *et al.*, 2013 A novel intronic single nucleotide polymorphism in the myosin heavy polypeptide 4 gene is responsible for the mini-muscle phenotype characterized by major reduction in hind-limb muscle mass in mice. Genetics 195: 1385–1395.

Kelly, S. A., P. P. Czech, J. T. Wight, K. M. Blank, and T. Garland, Jr., 2006 Experimental evolution and phenotypic plasticity of hindlimb bones in high-activity house mice. J. Morphol. 267: 360–374.

Kelly, S. A., F. R. Gomes, E. M. Kolb, J. L. Malisch, and T. Garland, Jr., 2017 Effects of activity, genetic selection and their interaction on muscle metabolic capacities and organ masses in mice. J. Exp. Biol. 220: 1038–1047.

Kelly, S. A., D. L. Nehrenberg, K. Hua, T. Garland, Jr., and D. Pomp, 2012 Functional genomic architecture of predisposition to voluntary exercise in mice: expression QTL in the brain. Genetics 191: 643–654.

Kelly, S. A., D. L. Nehrenberg, K. Hua, T. Garland, Jr., and D. Pomp, 2014 Quantitative genomics of voluntary exercise in mice: transcriptional analysis and mapping of expression QTL in muscle. Physiol. Genomics 46: 593–601.

Kelly, S. A., D. L. Nehrenberg, J. L. Peirce, K. Hua, B. M. Steffy *et al.*, 2010 Genetic architecture of voluntary exercise in an advanced intercross line of mice. Physiol. Genomics 42: 190–200.

Khan, A. A., and J. G. Quigley, 2013 Heme and FLVCR-related transporter families SLC48 and SLC49. Mol. Aspects Med. 34: 669–682.

Kida, Y., 2004 Chick Dach1 interacts with the Smad complex and Sin3a to control AER formation and limb development along the proximodistal axis. Development 131: 4179–4187.

Klaassen, R. V., J. Stroeder, F. Coussen, A.-S. Hafner, J. D. Petersen *et al.*, 2016 Shisa6 traps AMPA receptors at postsynaptic sites and prevents their desensitization during synaptic activity. Nat. Commun. 7:.

Kolb, E. M., S. A. Kelly, and T. Garland, Jr., 2013a Mice from lines selectively bred for high voluntary wheel running exhibit lower blood pressure during withdrawal from wheel access. Physiol. Behav. 112–113: 49–55.

Kolb, E. M., S. A. Kelly, K. M. Middleton, L. S. Sermsakdi, M. A. Chappell *et al.*, 2010 Erythropoietin elevates but not voluntary wheel running in mice. J. Exp. Biol. 213: 510–519.

Kolb, E. M., E. L. Rezende, L. Holness, A. Radtke, S. K. Lee *et al.*, 2013b Mice selectively bred for high voluntary wheel running have larger midbrains: support for the mosaic model of brain evolution. J. Exp. Biol. 216: 515–523.

Konczal, M., P. Koteja, P. Orlowska-Feuer, J. Radwan, E. T. Sadowska *et al.*, 2016 Genomic response to selection for predatory behavior in a mammalian model of adaptive radiation. Mol. Biol. Evol. 33: 2429–2440.

Koob, G. F., and N. D. Volkow, 2010 Neurocircuitry of Addiction. Neuropsychopharmacology 35: 217–238.

Kostrzewa, E., and M. J. Kas, 2014 The use of mouse models to unravel genetic architecture of physical activity: a review: Unravel genetic architecture of physical activity. Genes Brain Behav. 13: 87–103.

Köttgen, A., C. Pattaro, C. A. Böger, C. Fuchsberger, M. Olden *et al.*, 2010 New loci associated with kidney function and chronic kidney disease. Nat. Genet. 42: 376–384.

Kropff, E., J. E. Carmichael, M.-B. Moser, and E. I. Moser, 2015 Speed cells in the medial entorhinal cortex. Nature 523: 419–424.

Lachman, H. M., C. S. J. Fann, M. Bartzis, O. V. Evgrafov, R. N. Rosenthal *et al.*, 2007 Genomewide suggestive linkage of opioid dependence to chromosome 14q. Hum. Mol. Genet. 16: 1327–1334.

Lalley, P. M., R. Benacka, A. M. Bischoff, and D. W. Richter, 1997 Nucleus raphe obscurus evokes 5-HT-1A receptor-mediated modulation of respiratory neurons. Brain Res. 747: 156–159.

Lee, D., X. Zhao, Y.-I. Yim, E. Eisenberg, and L. E. Greene, 2008 Essential role of cyclin-G–associated kinase (auxilin-2) in developing and mature mice (R. Parton, Ed.). Mol. Biol. Cell 19: 2766–2776.

Li, J.-Y., T. B. J. Kuo, I.-T. Hsieh, and C. C. H. Yang, 2012 Changes in hippocampal theta rhythm and their correlations with speed during different phases of voluntary wheel running in rats. Neuroscience 213: 54–61.

Lightfoot, J. T., 2011 Current understanding of the genetic basis for physical activity. J. Nutr. 141: 526–530.

Lightfoot, J. T., E. J. C. De Geus, F. W. Booth, M. S. Bray, M. Den Hoed *et al.*, 2018 Biological/genetic regulation of physical activity level: Consensus from GenBioPAC. Med. Sci. Sports Exerc. 50: 863–873.

Lightfoot, J. T., L. Leamy, D. Pomp, M. J. Turner, A. A. Fodor *et al.*, 2010 Strain screen and haplotype association mapping of wheel running in inbred mouse strains. J. Appl. Physiol. 109: 623–634.

Lightfoot, J. T., M. J. Turner, D. Pomp, S. R. Kleeberger, and L. J. Leamy, 2008 Quantitative trait loci for physical activity traits in mice. Physiol. Genomics 32: 401–408.

Lillie, M., C. F. Honaker, P. B. Siegel, and Ö. Carlborg, 2019 Bidirectional selection for body weight on standing genetic variation in a chicken model. Genes|Genomes|Genetics g3.400038.2019.

Lin, X., C. B. Eaton, J. E. Manson, and S. Liu, 2017 The genetics of physical activity. Curr. Cardiol. Rep. 19:.

Liu, Q., R. J. Duff, B. Liu, A. L. Wilson, S. G. Babb-Clendenon *et al.*, 2006 Expression of cadherin10, a type II classic cadherin gene, in the nervous system of the embryonic zebrafish. Gene Expr. Patterns 6: 703–710.

Loh, N. Y., L. Bentley, H. Dimke, S. Verkaart, P. Tammaro *et al.*, 2013 Autosomal dominant hypercalciuria in a mouse model due to a mutation of the epithelial calcium channel, TRPV5 (Y. Ishimaru, Ed.). PLoS ONE 8: e55412.

Loos, R. J. F., T. Rankinen, A. Tremblay, L. Pérusse, Y. Chagnon *et al.*, 2005 Melanocortin-4 receptor gene and physical activity in the Québec Family Study. Int. J. Obes. 29: 420–428.

Machado, C. B., K. C. Kanning, P. Kreis, D. Stevenson, M. Crossley *et al.*, 2014 Reconstruction of phrenic neuron identity in embryonic stem cell- derived motor neurons. Development 141: 784–794.

Manley, A. F., 1996 *Physical activity and health: a report of the Surgeon General*. DIANE Publishing.

Mardon, G., N. M. Solomon, and G. M. Rubin, 1994 *dachshund* encodes a nuclear protein required for normal eye and leg development in *Drosophila*. Development 120: 3473–3486.

Martin, G. M., S. N. Austad, and T. E. Johnson, 1996 Genetic analysis of ageing: role of oxidative damage and environmental stresses. Nat. Genet. 13: 25–34.

Mathes, W. F., D. L. Nehrenberg, R. Gordon, K. Hua, T. Garland, Jr. *et al.*, 2010 Dopaminergic dysregulation in mice selectively bred for excessive exercise or obesity. Behav. Brain Res. 210: 155–163.

Matsunaga, E., S. Nambu, M. Oka, and A. Iriki, 2015 Complex and dynamic expression of cadherins in the embryonic marmoset cerebral cortex. Dev. Growth Differ. 57: 474–483.

Matta Mello Portugal, E., T. Cevada, R. Sobral Monteiro-Junior, T. Teixeira Guimarães, E. da Cruz Rubini *et al.*, 2013 Neuroscience of exercise: from neurobiology mechanisms to mental health. Neuropsychobiology 68: 1–14.

McGillivray, D. G., T. Garland, Jr., E. M. Dlugosz, M. A. Chappell, and D. A. Syme, 2009 Changes in efficiency and myosin expression in the small-muscle phenotype of mice selectively bred for high voluntary running activity. J. Exp. Biol. 212: 977–985.

Meek, T. H., B. P. Lonquich, R. M. Hannon, and T. Garland, Jr., 2009 Endurance capacity of mice selectively bred for high voluntary wheel running. J. Exp. Biol. 212: 2908–2917.

Miro, X., X. Zhou, S. Boretius, T. Michaelis, C. Kubisch *et al.*, 2009 Haploinsufficiency of the murine polycomb gene Suz12 results in diverse malformations of the brain and neural tube. Dis. Model. Mech. 2: 412–418.

Mok, A., K.-T. Khaw, R. Luben, N. Wareham, and S. Brage, 2019 Physical activity trajectories and mortality: population based cohort study. BMJ l2323.

Morgan, A. P., and C. E. Welsh, 2015 Informatics resources for the Collaborative Cross and related mouse populations. Mamm. Genome 26: 521–539.

Mosher, D. S., P. Quignon, C. D. Bustamante, N. B. Sutter, C. S. Mellersh *et al.*, 2007 A mutation in the myostatin gene increases muscle mass and enhances racing performance in heterozygote dogs (J. S. Takahashi, Ed.). PLoS Genet. 3: e79.

Myers, A., C. Gibbons, G. Finlayson, and J. Blundell, 2017 Associations among sedentary and active behaviours, body fat and appetite dysregulation: investigating the myth of physical inactivity and obesity. Br. J. Sports Med. 51: 1540–1544.

Neufer, P. D., M. M. Bamman, D. M. Muoio, C. Bouchard, D. M. Cooper *et al.*, 2015 Understanding the cellular and molecular mechanisms of physical activity-induced health benefits. Cell Metab. 22: 4–11.

Nica, A. C., and E. T. Dermitzakis, 2013 Expression quantitative trait loci: present and future. Philos. Trans. R. Soc. B Biol. Sci. 368: 20120362.

Nicod, J., R. W. Davies, N. Cai, C. Hassett, L. Goodstadt *et al.*, 2016 Genome-wide association of multiple complex traits in outbred mice by ultra-low-coverage sequencing. Nat. Genet. 48: 912–918.

Nogueira, A., O. Molinero, A. Salguero, and S. Márquez, 2018 Exercise addiction in practitioners of endurance sports: A literature review. Front. Psychol. 9:.

Nuwal, T., M. Kropp, S. Wegener, S. Racic, I. Montalban *et al.*, 2012 The *Drosophila* homologue of tubulin-specific chaperone E–like protein is required for synchronous sperm individualization and normal male fertility. J. Neurogenet. 26: 374–381.

Pallafacchina, G., S. François, B. Regnault, B. Czarny, V. Dive *et al.*, 2010 An adult tissue-specific stem cell in its niche: A gene profiling analysis of in vivo quiescent and activated muscle satellite cells. Stem Cell Res. 4: 77–91.

Park, S., and J. L. Etnier, 2019 Beneficial effects of acute exercise on executive function in adolescents. J. Phys. Act. Health 16: 423–429.

Parker, C. C., S. Gopalakrishnan, P. Carbonetto, N. M. Gonzales, E. Leung *et al.*, 2016 Genome-wide association study of behavioral, physiological and gene expression traits in outbred CFW mice. Nat. Genet. 48: 919–926.

1276 Parker, C. C., and A. A. Palmer, 2011 Dark Matter: Are mice the solution to missing heritability? Front.
1277 Genet. 2:.
1278 Prince, S. A., K. B. Adamo, M. Hamel, J. Hardt, S. Connor Gorber *et al.*, 2008 A comparison of direct
1279 versus self-report measures for assessing physical activity in adults: a systematic review. Int. J.
1280 Behav. Nutr. Phys. Act. 5: 56.
1281 Rendeiro, C., and J. S. Rhodes, 2018 A new perspective of the hippocampus in the origin of exercise–
1282 brain interactions. Brain Struct. Funct. 223: 2527–2545.
1283 Rezende, E. L., F. R. Gomes, J. L. Malisch, M. A. Chappell, and T. Garland, Jr., 2006 Maximal oxygen
1284 consumption in relation to subordinate traits in lines of house mice selectively bred for high
1285 voluntary wheel running. J. Appl. Physiol. 101: 477–485.
1286 Rhodes, J. S., S. C. Gammie, and T. Garland Jr, 2005 Neurobiology of mice selected for high voluntary
1287 wheel-running activity. Integr. Comp. Biol. 45: 438–455.
1288 Rhodes, J. S., and T. Garland, Jr., 2003 Differential sensitivity to acute administration of Ritalin,
1289 apormorphine, SCH 23390, but not raclopride in mice selectively bred for hyperactive wheel-
1290 running behavior. Psychopharmacology (Berl.) 167: 242–250.
1291 Rhodes, J. S., T. Garland, Jr., and S. C. Gammie, 2003a Patterns of brain activity associated with variation
1292 in voluntary wheel-running behavior. Behav. Neurosci. 117: 1243–1256.
1293 Rhodes, J. S., G. R. Hosack, I. Girard, A. E. Kelley, G. S. Mitchell *et al.*, 2001 Differential sensitivity to acute
1294 administration of cocaine, GBR 12909, and fluoxetine in mice selectively bred for hyperactive
1295 wheel-running behavior. Psychopharmacology (Berl.) 158: 120–131.
1296 Rhodes, J. S., H. van Praag, S. Jeffrey, I. Girard, G. S. Mitchell *et al.*, 2003b Exercise increases
1297 hippocampal neurogenesis to high levels but does not improve spatial learning in mice bred for
1298 increased voluntary wheel running. Behav. Neurosci. 117: 1006–1016.

Roberts, M. D., G. N. Ruegsegger, J. D. Brown, and F. W. Booth, 2017 Mechanisms associated with physical activity behavior: insights from rodent experiments. Exerc. Sport Sci. Rev. 45: 217–222.

Rohe, M., 2008 Role of SORLA in the brain and its relevance for Alzheimer disease [Ph.D. Dissertation]: Freien Universität Berlin, 110 p.

van Rooij, E., D. Quiat, B. A. Johnson, L. B. Sutherland, X. Qi *et al.*, 2009 A family of microRNAs encoded by myosin genes governs myosin expression and muscle performance. Dev. Cell 17: 662–673.

Rosenfeld, C. S., 2017 Sex-dependent differences in voluntary physical activity: Physical Activity and Sex Differences. J. Neurosci. Res. 95: 279–290.

Rowland, T., 2016 *Biologic regulation of physical activity*. Human Kinetics Publishers.

Saiga, T., T. Fukuda, M. Matsumoto, H. Tada, H. J. Okano *et al.*, 2009 Fbxo45 forms a novel ubiquitin ligase complex and is required for neuronal development. Mol. Cell. Biol. 29: 3529–3543.

Salsi, V., M. A. Vigano, F. Cocchiarella, R. Mantovani, and V. Zappavigna, 2008 Hoxd13 binds in vivo and regulates the expression of genes acting in key pathways for early limb and skeletal patterning. Dev. Biol. 317: 497–507.

Sarzynski, M. A., R. J. F. Loos, A. Lucia, L. Pérusse, S. M. Roth *et al.*, 2016 Advances in exercise, fitness, and performance genomics in 2015: Med. Sci. Sports Exerc. 48: 1906–1916.

Saul, M. C., P. Majdak, S. Perez, M. Reilly, T. Garland, Jr. *et al.*, 2017 High motivation for exercise is associated with altered chromatin regulators of monoamine receptor gene expression in the striatum of selectively bred mice: Striatal transcriptome of mice born to run. Genes Brain Behav. 16: 328–341.

Schiller, D., H. Eichenbaum, E. A. Buffalo, L. Davachi, D. J. Foster *et al.*, 2015 Memory and space: towards an understanding of the cognitive map. J. Neurosci. 35: 13904–13911.

Schmidt, V., A. Subkhangulova, and T. E. Willnow, 2017 Sorting receptor SORLA: cellular mechanisms and implications for disease. Cell. Mol. Life Sci. 74: 1475–1483.

Schwartz, N. L., B. A. Patel, T. Garland, Jr., and A. M. Horner, 2018 Effects of selective breeding for high voluntary wheel-running behavior on femoral nutrient canal size and abundance in house mice. J. Anat. 233: 193–203.

Secades, J., and J. Lorenzo, 2006 Citicoline: pharmacological and clinical review, 2006 update. Methods Find Exp Clin Pharmacol 28 Suppl B: 1–56.

Sella, G., and N. H. Barton, 2019 Thinking about the evolution of complex traits in the era of genome-wide association studies. Annu. Rev. Genomics Hum. Genet. 20: 461–493.

Sellami, M., M. Gasmi, J. Denham, L. D. Hayes, D. Stratton *et al.*, 2018 Effects of acute and chronic exercise on immunological parameters in the elderly aged: can physical activity counteract the effects of aging? Front. Immunol. 9:.

Sheel, A. W., 2016 Sex differences in the physiology of exercise: an integrative perspective: Introduction. Exp. Physiol. 101: 211–212.

Sheila, M., G. Narayanan, S. Ma, W. L. Tam, J. Chai *et al.*, 2019 Phenotypic and molecular features underlying neurodegeneration of motor neurons derived from spinal and bulbar muscular atrophy patients. Neurobiol. Dis. 124: 1–13.

Shen, Y., Z. Ding, S. Ma, Z. Ding, Y. Zhang *et al.*, 2019 SETD7 mediates spinal microgliosis and neuropathic pain in a rat model of peripheral nerve injury. Brain. Behav. Immun. 82: 382–395.

Sheremet, A., J. P. Kennedy, Y. Qin, Y. Zhou, S. D. Lovett *et al.*, 2019 Theta-gamma cascades and running speed. J. Neurophysiol. 121: 444–458.

Shim, H., H. Chun, C. D. Engelman, and B. A. Payseur, 2009 Genome-wide association studies using single-nucleotide polymorphisms versus haplotypes: an empirical comparison with data from the North American Rheumatoid Arthritis Consortium. BMC Proc. 3: S35.

Shimomura, K., 2001 Genome-wide epistatic interaction analysis reveals complex genetic determinants of circadian behavior in mice. Genome Res. 11: 959–980.

1347 Simonen, R. L., T. Rankinen, L. Pérusse, A. S. Leon, J. S. Skinner *et al.*, 2003 A dopamine D2 receptor gene
1348 polymorphism and physical activity in two family studies. Physiol. Behav. 78: 751–757.
1349 Singleton, J. M., and T. Garland, Jr., 2019 Influence of corticosterone on growth, home-cage activity,
1350 wheel running, and aerobic capacity in house mice selectively bred for high voluntary wheel-
1351 running behavior. Physiol. Behav. 198: 27–41.
1352 Smits, P., P. Li, J. Mandel, Z. Zhang, J. M. Deng *et al.*, 2001 The transcription factors L-Sox5 and Sox6 are
1353 essential for cartilage formation. Dev. Cell 1: 277–290.
1354 Stoltenberg, S. F., M. K. Lehmann, C. C. Christ, S. L. Hersrud, and G. E. Davies, 2011 Associations among
1355 types of impulsivity, substance use problems and Neurexin-3 polymorphisms. Drug Alcohol
1356 Depend. 119: e31–e38.
1357 Swallow, J. G., T. Garland, Jr., P. A. Carter, W.-Z. Zhan, and G. C. Sieck, 1998 Effects of voluntary activity
1358 and genetic selection on aerobic capacity in house mice (*Mus domesticus*). J. Appl. Physiol. 84:
1359 69–76.
1360 Swallow, J. G., P. Koteja, P. A. Carter, and T. Garland Jr., 2001 Food consumption and body composition
1361 in mice selected for high wheel-running activity. J. Comp. Physiol. [B] 171: 651–659.
1362 Swallow, J. G., J. S. Rhodes, and T. Garland Jr, 2005 Phenotypic and evolutionary plasticity of organ
1363 masses in response to voluntary exercise in house mice. Integr. Comp. Biol. 45: 426–437.
1364 Tada, H., H. J. Okano, H. Takagi, S. Shibata, I. Yao *et al.*, 2010 Fbxo45, a novel ubiquitin ligase, regulates
1365 synaptic activity. J. Biol. Chem. 285: 3840–3849.
1366 Taliun, D., J. Gamper, U. Leser, and C. Pattaro, 2016 Fast sampling-based whole-genome haplotype block
1367 recognition. IEEE/ACM Trans. Comput. Biol. Bioinform. 13: 315–325.
1368 Talmadge, R. J., W. Acosta, and T. Garland, Jr., 2014 Myosin heavy chain isoform expression in adult and
1369 juvenile mini-muscle mice bred for high-voluntary wheel running. Mech. Dev. 134: 16–30.

Thomas, J. R., and K. T. Thomas, 1988 Development of gender differences in physical activity. Quest 40: 219–229.

Thompson, Z., 2017 The neurobiological basis of voluntary exercise in selectively-bred high runner mice: University of California, Riverside, 150 p.

Thompson, Z., D. Argueta, T. Garland, Jr., and N. DiPatrizio, 2017 Circulating levels of endocannabinoids respond acutely to voluntary exercise, are altered in mice selectively bred for high voluntary wheel running, and differ between the sexes. Physiol. Behav. 170: 141–150.

Vaanholt, L. M., I. Jonas, M. Doornbos, K. A. Schubert, C. Nyakas *et al.*, 2008 Metabolic and behavioral responses to high-fat feeding in mice selectively bred for high wheel-running activity. Int. J. Obes. 32: 1566–1575.

Vann, S. D., J. P. Aggleton, and E. A. Maguire, 2009 What does the retrosplenial cortex do? Nat. Rev. Neurosci. 10: 792–802.

Walker, E. P., and P. Tadi, 2020 Neuroanatomy, Nucleus Raphe, in *Neuroanatomy, Nucleus Raphe*, StatPearls Publishing.

Wallace, I. J., and T. Garland, Jr., 2016 Mobility as an emergent property of biological organization: Insights from experimental evolution: Mobility and biological organization. Evol. Anthropol. Issues News Rev. 25: 98–104.

Wang, W., K. K. Touhara, K. Weir, B. P. Bean, and R. MacKinnon, 2016 Cooperative regulation by G proteins and Na+ of neuronal GIRK2 K+ channels. eLife 5:.

White, J. K., A.-K. Gerdin, N. A. Karp, E. Ryder, M. Buljan *et al.*, 2013 Genome-wide generation and systematic phenotyping of knockout mice reveals new roles for many genes. Cell 154: 452–464.

Williams, C. J., M. G. Williams, N. Eynon, K. J. Ashton, J. P. Little *et al.*, 2017 Genes to predict VO2max trainability: a systematic review. BMC Genomics 18:.

1393 Wise, R. A., 2009 Roles for nigrostriatal—not just mesocorticolimbic—dopamine in reward and
1394 addiction. Trends Neurosci. 32: 517–524.
1395 Wolock, S. L., A. Yates, S. A. Petrill, J. W. Bohland, C. Blair *et al.*, 2013 Gene × smoking interactions on
1396 human brain gene expression: finding common mechanisms in adolescents and adults. J. Child
1397 Psychol. Psychiatry 54: 1109–1119.
1398 Wood, A. R., The Electronic Medical Records and Genomics (eMERGE) Consortium, The MIGen
1399 Consortium, The PAGE Consortium, The LifeLines Cohort Study *et al.*, 2014 Defining the role of
1400 common variation in the genomic and biological architecture of adult human height. Nat. Genet.
1401 46: 1173–1186.
1402 Xu, S., and T. Garland, 2017 A mixed model approach to genome-wide association studies for selection
1403 signatures, with application to mice bred for voluntary exercise behavior. Genetics 207: 785–
1404 799.
1405 Xu, Y., X.-M. Zhao, J. Liu, Y.-Y. Wang, L.-L. Xiong *et al.*, 2020 Complexin I knockout rats exhibit a complex
1406 neurobehavioral phenotype including profound ataxia and marked deficits in lifespan. Pflüg.
1407 Arch. - Eur. J. Physiol. 472: 117–133.
1408 Yang, Z., Q. Sun, J. Guo, S. Wang, G. Song *et al.*, 2019 *GRSF1* -mediated *MIR-G-1* promotes malignant
1409 behavior and nuclear autophagy by directly upregulating *TMED5* and *LMNB1* in cervical cancer
1410 cells. Autophagy 15: 668–685.
1411 Ye, J., M. P. Witter, M.-B. Moser, and E. I. Moser, 2018 Entorhinal fast-spiking speed cells project to the
1412 hippocampus. Proc. Natl. Acad. Sci. 115: E1627–E1636.
1413 Young, N. M., B. Hallgrímsson, and T. Garland, Jr., 2009 Epigenetic effects on integration of limb lengths
1414 in a mouse model: selective breeding for high voluntary locomotor activity. Evol. Biol. 36: 88–99.

Zheng, J.-J., W.-X. Li, J.-Q. Liu, Y.-C. Guo, Q. Wang *et al.*, 2018 Low expression of aging-related NRXN3 is associated with Alzheimer disease: A systematic review and meta-analysis. Medicine (Baltimore) 97: e11343.

Zhu, X., E.-S. Cho, Q. Sha, J. Peng, Y. Oksov *et al.*, 2014 Giant axon formation in mice lacking Kell, XK, or Kell and XK. Am. J. Pathol. 184: 800–807.

Zhu, X., A. Rivera, M. S. Golub, J. Peng, Q. Sha *et al.*, 2009 Changes in red cell ion transport, reduced intratumoral neovascularization, and some mild motor function abnormalities accompany targeted disruption of the Mouse Kell gene (*Kel*). Am. J. Hematol. 84: 492–498.